

© 2011 by Rekha C. Balachandran. All rights reserved.

BUILDING A ROBUST BACTERIAL CHASSIS FOR
SYNTHETIC BIOLOGY

BY

REKHA C. BALACHANDRAN

THESIS

Submitted in partial fulfillment of the requirements
for the degree of Master of Science in Agricultural and Biological Engineering
in the Graduate College of the
University of Illinois at Urbana-Champaign, 2011

Urbana, Illinois

Master's Committee:

Associate Professor Kaustubh Bhalerao
Assistant Professor Charles Schroeder
Assistant Professor Luis Rodríguez

Abstract

Stress response mechanisms in bacteria helps them sustain stressful and competitive environments caused by nutrient limitation. Often these stresses give rise adaptive phenotypes that are evolutionarily fitter under nutrient limitation. These phenotypes possess favorable adaptations that help them scavenge and recycle amino acids, carbohydrates, and lipids from other cells, thus playing a crucial role in their survival.

The objective of this project was to develop a systematic procedure to produce evolutionarily fitter populations of *E.coli* to test the following hypotheses - (1) Bacteria that show increased fitness after being subjected to stress and can outcompete their naïve counterparts in a limited resource environment. (2) This increased competitiveness could be exploited to develop a new class of metabolically efficient, contamination resistant host organisms for industrial biotechnology.

E.coli cultures were exposed to a nutritionally stressful scenario by aging them in fed-batch cultures. Upon competing the aged cultures with the naïve ones it was observed that the aged cultures prevail over the naïve ones. This is due to a previously observed phenomenon called Growth Advantage in Stationary Phase (GASP), which is believed to be the result of beneficial physiological changes in cells due to imposed nutritional stress.

The metabolic burden imposed on the cells was measured by calculating the doubling time. The doubling time served as a proxy for calculating the fitness of

stress hardened cells. Metabolic burden for cells containing plasmids and cells where this plasmid was integrated on the chromosome was measured to characterize the relative metabolic advantage of the integrands over cells with. It was observed that the cells with plasmids experienced higher metabolic burden.

Heterologous protein expression in the stress hardened cells was analyzed to determine if the physiological changes influence protein expression. GFP was used for testing the protein expression. The stress hardened cells showed an approximate two fold increase in the expression of GFP which was a surprising result as the increased production of GFP is not beneficial for the cell in itself.

The stress hardened GASP phenotypes could be used as a chassis for producing commercially relevant proteins and antibiotics. The GASP phenotype is contamination resistant as it is capable of surviving in a nutrient limited condition. This phenotype shows slower growth rate and increased protein production implying that these cells could produce more product for the same amount of materials hence reducing the production cost. Thus, the GASP phenotype could serve a robust chassis for synthetic biology because of the beneficial adaptations it acquires.

For my father who taught me perseverance

Acknowledgments

Moving to Champaign-Urbana in Spring of 2009 to start my graduate studies has been the most exciting part of my life. It was an adventure in every sense - new places new people and most importantly exciting work.

Dr. Kaustubh Bhalerao, my advisor has been a constant source of inspiration. Together we embarked upon a challenging project for my master's which has been a roller coaster ride. He showed faith in me even during the times when nothing would work right. Our discussions would always leave me motivated and filled with ideas. It is because of his unwavering support that I am at the culmination of my M.S research project. I am indebted to him for putting me on this project which gave me sleepless nights and immense joy in figuring out solutions for the problems we encountered along the way.

I would also like to thank Dr. Steven R. Eckhoff for teaching me that every question is important. I would like to express my gratitude for his help and support through one of the most difficult times in my life. I would like to thank Dr. Charles Schroeder and Dr. Luis Rodríguez for serving my committee, providing invaluable suggestions and guiding me successfully towards completing my project.

I would also like to thank Dr. Barbara Pilas and Ben Montez at the Flow Cytometry Facility for helping me. I am grateful to Vaisak Parekatt for being the best lab mate ever. Arnab Mukherjee taught me that life is non-linear and good things come to people who do good science. I am thankful to him for all the help I

got from him for research and as a friend. I thank Dr. Goutam Nistala for helping me. I am also grateful to all my friends at Illinois who helped me relax so that I could work with more vigor.

Last but not least I thank my sister Dr. Malini Iyer for teaching me that sky is not the limit and my parents for their unfaltering love and support and believing in me. I would like to thank Jay Krishnamoorthy for all the advice and support that got me through the rough patches. I would also like to thank Bhushan Mahadik for all the help and support.

Table of Contents

List of Figures	ix
List of Tables	x
Chapter 1 Introduction and Literature Review	1
1.1 Synthetic biology	1
1.1.1 Applications of synthetic biology	7
1.2 Metabolic burden in synthetic gene circuits	9
1.3 Physiological changes in a cell culture in response to metabolic burden	12
1.4 Specific aims of the project	15
Chapter 2 Materials and Methods	17
2.1 Growth conditions and media	17
2.2 Experimental methods and protocols	18
2.2.1 Absorbance and fluorescence assays	18
2.2.2 Fluorescence Activated Cell Sorting (FACS)	19
2.2.3 The <i>LacZ</i> competition experiment	19
2.2.4 Construction and aging of DH5 α cells for competition assay	22
2.2.5 Competition assay	23
2.2.6 Construction of cells with plasmids integrated in chromosome	26
2.2.7 Heterologous protein expression in GASP phenotype	27
Chapter 3 Results and Discussion	33
3.1 Reproducing the GASP phenomenon	33
3.1.1 <i>LacZ</i> competition experiment	33
3.1.2 Quantification of competitive advantage of GASP phenotype	37
3.2 Analysis of metabolic burden	40
3.3 Heterologous protein expression in GASP phenotypes	42
3.3.1 Spectrophotometric analysis	42
3.3.2 Western blot	43
3.3.3 FACS analysis	44

3.4	Conclusions	46
Chapter 4	Future prospects	47
References	48

List of Figures

1.1	Toggle switch design	4
1.2	Repressilator design	5
1.3	Positive feedback amplifier	6
1.4	Oscillations in the dual- feedback circuit	6
1.5	Types of synthetic manipulation in genetic circuits	10
1.6	Behaviour of synthetic circuits in long-term experiments.	11
1.7	Growth curve graphs	13
1.8	Dynamic emergence of GASP phenotypes	14
2.1	Action of β galactosidase	20
2.2	Plasmid map of mCherry.	24
2.3	Plasmid map of pVenus.	25
2.4	Plasmid map of PROTet 6x HN with GFP.	29
2.5	Assembly of the cassette for western blot.	30
3.1	Colorimetric analysis of Xgal metabolism	34
3.2	Calibration of Time	34
3.3	Proportion of <i>LacZ</i> cells in 50% X-gal	35
3.4	Competition assay results for <i>lacZ</i> cells	35
3.5	Screening for GASP phenotype	36
3.6	Competition assay results for DH5 α cells with fluorescent proteins	38
3.7	Doubling time calculated based on the Logistic growth model	40
3.8	Growth curve of GASP phenotypes expressing GFP	42
3.9	Spectrophotometric Analysis heterologous protein expression	43
3.10	Quantitative western blot	44
3.11	FACS analysis	45

List of Tables

2.1	Luria - Bertani broth	17
2.2	5x M9 Minimal Media	18
2.3	1x M9 Minimal Media	18
2.4	Antibiotics	18
3.1	Fold increase in expression	45

Chapter 1

Introduction and Literature Review

1.1 Synthetic biology

The rise of biotechnology and biomolecular engineering depends on the ability to efficiently manipulate gene sequences using polymerases, restriction endonucleases and ligases to create novel functional genetic constructs for applications ranging from healthcare to recombinant enzyme production. For last 30 years, this field has been almost exclusively devoted to cloning recombinant genes with a view of creating microbial cell factories. More recently an engineering approach to biotechnology has driven the field towards assembling cellular systems from well-characterized biological parts with reliable and predictable outcomes (1; 2). The focus has shifted from importing mere functionality into the cell to importing the associated spatial and temporal controls of the functionality. The progress in this field has been helped by the reduction in cost of chemical DNA synthesis and the use of model-guided circuit assembly that aids rapid construction and evaluation of genetic circuits (3).

Synthetic biology is formally defined as the design and fabrication of biological components and systems that do not already exist in the natural world and / or the re-design and fabrication of existing biological systems (www.syntheticbiology.org).

The foundational principles of design in synthetic biology espouse common engineering practices such as abstraction, standardization and modularization.

Abstraction is a method by which complex information is hidden for practical purposes by representing it with readily comprehensible linguistic or graphical notations. Abstractions highlight information relevant to functionality of a biological molecule while hiding details such as its structure, which have limited relevance to using the biomolecule. At this level the synthetic biologist is concerned only with the system hierarchy such as parts and devices. The hierarchy is organized in such way that there is only limited and required exchange of information between parts, devices, and systems (4). Abstraction enables decoupling design from construction. The ultimate goal of synthetic biology is to be able to design synthetic system with predictable behavior and high levels of abstraction using the engineering tools available (5).

Engineering biology depends on design, abstraction and design decoupling which leads to standardization of biological parts. These parts are therefore required to be both physically and functionally reliable (6; 7). The registry of standard biological parts, BioBricksTM, housed at Massachusetts Institute of Technology is a collection of standardized biological parts that encode for the promoters, terminators, enzymes, activators, repressors, reporters, and ribosome binding sites (Registry of Standard Biological Parts, 2010). Prototypes of genetic devices can be created quickly with the help of the standardized parts from BioBricksTM (8; 9). Individual parts that fail to function as per the design requirements can be identified and replaced easily with ones that function and fit the design after rigorous testing and characterization (10). Parallel assembly of higher order devices can improve the development of synthetic gene circuits (11).

The International Genetically Engineered Machine (iGEM) is a worldwide competition aimed at promoting synthetic biology ideas in undergraduate programs. The undergraduate teams are provided with a kit of biological parts from the Registry. The students work towards designing and building biological

systems and testing them in living cells using these parts and new parts designed by them. The vision behind the Parts Registry is for it to serve as a resource for synthetic biologists. The synthetic biologists would design a system comprising of numerous biochemical processes and then implement the design with well characterized parts using standardized methods of assembly. The behavior of this device is characterized to produce a datasheet. This datasheet is used as an interface between the engineers and the device (7; 12).

One of the earliest demonstrations of synthetic biology was the genetic toggle switch by Gardner *et al* (13). This circuit could control gene expression between on and off states depending on the external stimuli. This synthetic genetic toggle switch employs a pair of promoters encoding mutually repressing regulators. This mutual repression is analogous to the lysis-lysogeny switch observed in bacteriophage λ . This bacteriophage λ has two promoters that mutually repress the gene product of the other thus helping the organism to switch between the lysis and lysogeny states of bacteriophage infection (14). The P_L promoter from the bacteriophage λ was used with lacI repressor to repress the P_{trc2} promoter. The P_{trc2} promoter controlled the expression of the temperature sensitive Cl-ts gene that translates into the λ Cl repressor protein which in turn represses the P_L promoter. The third variant used the $P_{LtetO-1}$ promoter with Tet repressor. The system was manipulated using two different exogenous signals in order to activate gene production from each promoter and expression could be toggled between them. When one of the signals was removed, the system retained its current state, thus satisfying all the requirements of a toggle switch (13).

At the same time, Elowitz and colleagues developed a genetic oscillator circuit where three transcriptional repressors, each repressing the next were assembled to give rise to oscillations in the levels of transcriptional factors produced (15). LacI protein represses the transcription of the tetR gene from

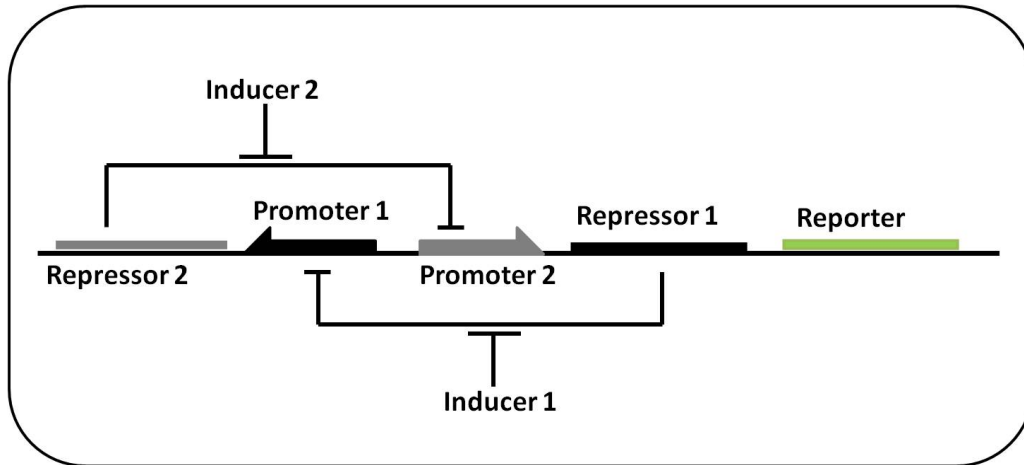


Figure 1.1. Toggle switch design.

Repressor 1 inhibits transcription from Promoter 1 and is induced by Inducer 1. Repressor 2 inhibits transcription from Promoter 2 and is induced by Inducer 2 (13).

tetracycline resistant transposon *Tn10*. This protein product in turn represses the transcription of the CI protein from bacteriophage λ , which in turn represses the *lacI* expression under the first promoter. This transcriptional activity was measured by green fluorescent protein expression on a separate reporter plasmid (15).

More recent examples of synthetic gene circuits include modular positive feedback-based gene amplifier comprising of a Taz sensor kinase and an OmpR regulator as shown in Figure 1.3 (16; 17). Aspartate, the inducer molecule binds to the Taz sensor kinase and causes OmpR to autophosphorylate which in turn activates OmpC promoter expressing LuxR (18). This in turn triggers the activity of pLuxI promoter expressing a LuxR-GFP construct. The signal from LuxR-GFP further up regulates the activity of its own promoter thereby making it behave in a positive feedback loop (19).

Another example of a tunable synthetic gene circuit for amplifying cellular oscillations is shown in Figure 1.4 (20; 21). The circuit was constructed using a hybrid promoter ($P_{lac/ara-1}$). This promoter is composed of the activation site

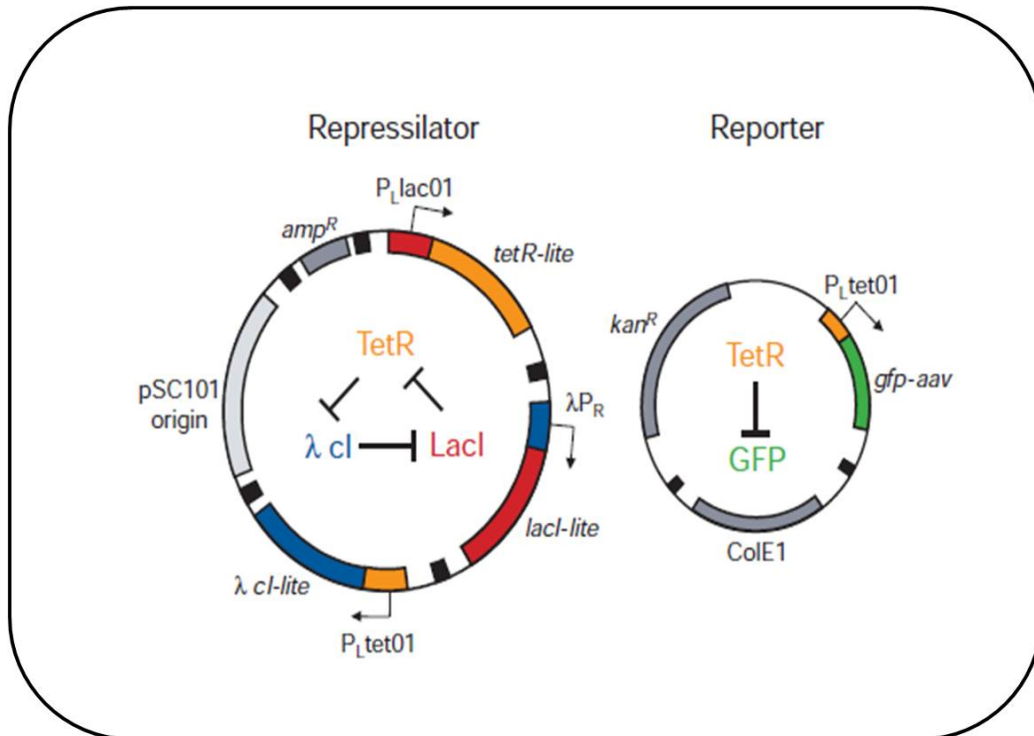


Figure 1.2. Repressilator design.

A cyclic negative feedback loop comprised of three repressor genes with their respective promoters (15).

from *araBAD* operon and the repression sequence from *lacZYA* operon (22). AraC protein activates the promoter in the presence of arabinose and LacI represses it in the absence of isopropyl β -D-1-thiogalactopyranoside (IPTG). AraC, LacI and a monomeric yeast-enhanced green fluorescent protein (*yemGFP*) reporter were placed under three identical copies of $P_{lac/ara-1}$ promoter to give rise to co-regulated transcription modules. In the presence of arabinose and IPTG the promoters transcribes the elements under their control. There is an increased production of AraC, as it is in a positive feedback loop. The increase in the production of LacI triggers the negative feedback loop, thereby decreasing the promoter activity. This differential activity between the two feedback loops results in oscillatory behavior. This circuit designed by Stricker *et al* (21) is an improved version of the oscillatory circuit designed by

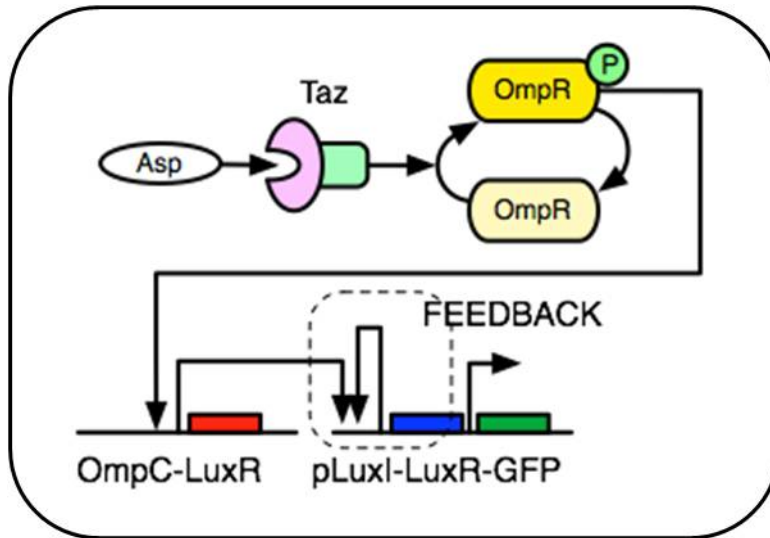


Figure 1.3. Positive feedback amplifier.

The two-component sensor consists of the Taz sensor kinase and the OmpR response regulator. Taz controls the level of phosphorylated OmpR (OmpR-P), which in turn activates the expression from the OmpC promoter. When the Taz sensor kinase is bound with aspartate, it increases the levels of OmpR-P, leading to increased expression from the OmpC promoter (16).

Elowitz *et al* (15) where the former is capable of tuning the oscillations in the circuit based on external stimuli.

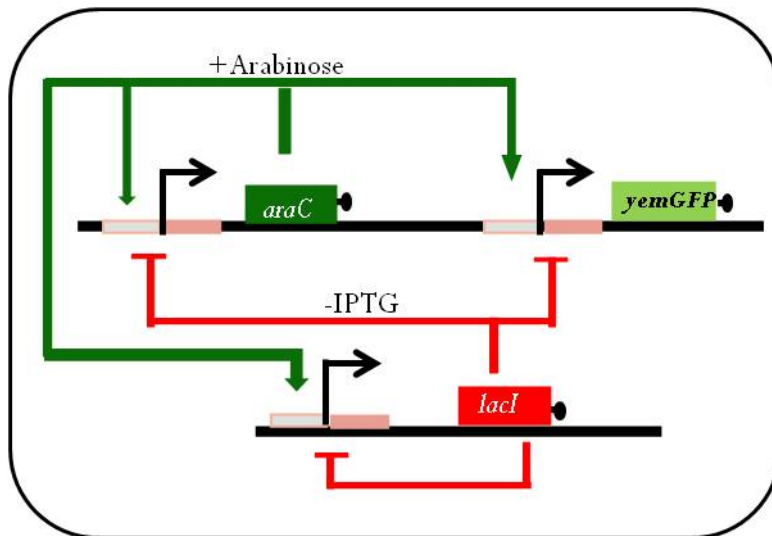


Figure 1.4. Oscillations in the dual-feedback circuit.

Hybrid promoter $P_{lac/ara-1}$ controls transcription of *araC* and *lacI* forming a positive and negative feedback loops (20).

1.1.1 Applications of synthetic biology

Synthetic biology could potentially address universal challenges like energy security, bioremediation, improving health, and increasing food and agriculture yields. Successful implementation of these applications could revolutionize the world. Some of the examples of the application of synthetic biology are recounted below.

Energy

Mycoplasma laboratorium is a partially synthetic species derived from the genome of *Mycoplasma genitalium*. This was the first of its kind synthetic organism created at the J. Craig Venter Institute (23). In an approach significantly distinct from engineering microorganisms for biofuel production it has been speculated that organisms that can produce biofuel can be created *de novo*. *M.laboratorium* has the potential to be exploited for biofuel production.

LS9 uses principles from synthetic biology and metabolic engineering to design and build biosynthetic pathways. They have successfully exploited microbial fatty acid metabolism to produce various fuels at a commercial level. They are currently collaborating with Chevron.inc to develop a sustainable hydrocarbon diesel product (<http://www.ls9.com>).

Microbial production of butanol via *Clostridium acetobutylicum* produces extremely low yields of butanol mixed with acetone and ethanol (24). To increase the yield of butanol standard fermentation pathways in *Clostridium acetobutylicum* were bypassed and a set of 2-keto acid intermediates of *E. coli* amino acid biosynthesis were synthetically shunted to increment the yields of butanol in two enzymatic steps (25).

Environment

Synthetic biology has also found application in the field of bioremediation. Atrazine which is present in most commercially used herbicides often seeps in to potable water. *E. coli* has been engineered to consume atrazine and degrade it to less harmful products. The by-products and bacteria can both be recycled (26). *Pseudomonas aeruginosa* can be used for bioremediation of 2-chlorotoluene . A hybrid pathway has been built in *P. aeruginosa* to degrade 2-chlorotoulune CO₂ and chloride (27; 28). Biosensors to detect arsenic, mercury, chromium and other such hazardous pollutants are being developed (29). *E. coli* cells have been engineered to fluoresce after contact with arsante or arsenite. This biosensor could consistently differentiate concentrations of 10-50 μg arsenite per liter of drinking water (29).

Health

De novo construction of mevalonate pathway in *E. coli* has improved the production of a precursor to artemisinin, an anti-malarial drug (30; 31; 32). These precursors were earlier extracted from the bark of *Artemisia annua* which greatly limited the drug production. With *E. coli* as the host organism production of the drug could be scaled-up while simultaneously decreasing the production time. The decrease in production time and scale up of the drug directly affected the cost of the drug, making it cheaper.

Nonlytic M13 bacteriophages were engineered to produce synthetic adjuvants to enhance the killing efficacy of the antibiotics. This method disturbed the existing defense mechanisms that bacteria have for antibiotic defense (33; 34).

Cancer invading bacteria were designed to target specific tumorigenic

pathways in vivo using RNAi (35). The bacteria were designed to knock down the expression of CTNNB1 (β -1 catenin) gene which initiates colon cancer. The bacteria generated short hairpin RNA (shRNA) segments that induced cleavage of the CTNNB1 mRNA transcripts. In addition to shRNA, the bacteria also possessed a synthetic system that enabled molecular efflux (35).

Food and agriculture

The 2011 iGEMTM team from Yale developed an antifreeze protein (AFP) from a Siberian beetle called *Rhagium inquisitor* that could prevent formation of ice crystals. Antifreeze proteins could be used for cryopreservation of food and for extending the crop growing seasons. The team employed protein engineering by directed evolution to evolve novel variants of the AFP (<http://2011.igem.org/Team:Yale/Project/Introduction>). They quantified the protein expression, purified it, and then subjected it to directed evolution thereby cloning three new variants. MAGE (multiplex automated genome engineering) was used for creating diversity in sequences over a large population of cells by an oligo mediated allelic replacement (36). AFP from *Rhagium inquisitor* (RiAFP) bears no homology to the antifreeze proteins from fish which are currently used as RiAFP has only one disulfide bond hence is less tightly folded. Being a small protein (136 amino acids) it was easily produced in *E. coli*.

1.2 Metabolic burden in synthetic gene circuits

Synthetic biology offers a bottom up approach to understanding and building gene circuits from well characterized components (37; 38; 39; 40; 41). The aforementioned circuits exemplify model guided bottom-up assembly of gene circuits as a key paradigm in synthetic biology design. However, the field is still

far from its goal of creating standardized and autonomous biological circuit design that could function robustly, independent of native gene networks or even functionally substitute endogenous circuitry altogether (42).

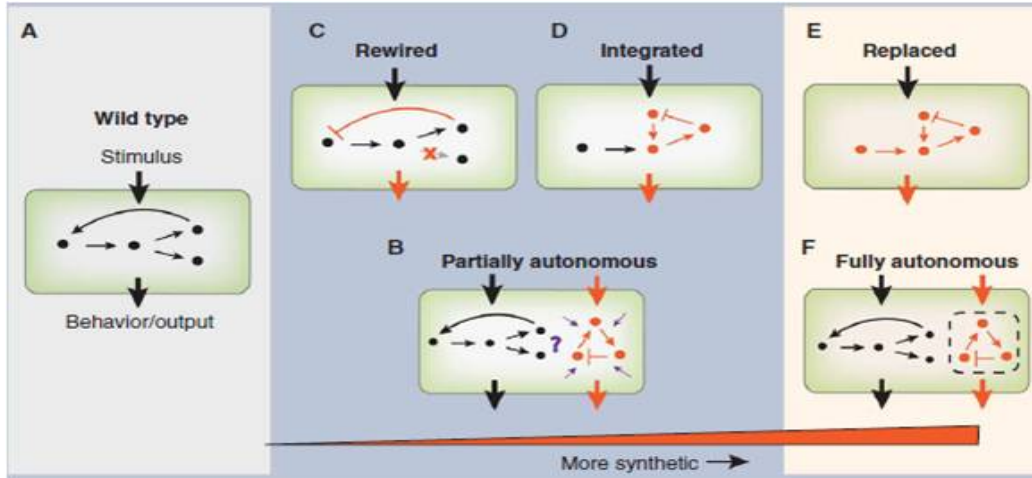


Figure 1.5. Types of synthetic manipulation in genetic circuits.

(A) Wild type cells can be modified in two ways. (C) Rewiring the cell's innate circuitry to perform the desired function. (D) Integrating a synthetic network in the cells innate circuitry to perform the same function. (E) The original network in the cell is replaced completely by a synthetic circuit. (B) Introducing a synthetic network in addition to the cell's innate network. (F) Introducing a fully autonomous circuit that operates independently of the cellular milieu (43).

Emerging scholarship suggests a classification system for evaluating increased complexity in Figure 1.5. The authors suggest that the circuit depicted in Figure 1.5 (F) (43) suggests an ideal scenario where the synthetic gene circuit introduced would be completely autonomous and be independent of the native cellular network and would have no interactions with the cells innate network.

In the process of modifying cells synthetically, cells are often assumed to be static black box which belies the complexity of the system. This assumption of treating the cell like a black box ignores the inevitable effects of cells' innate circuitry has on the synthetic network and vice versa. This assumption of decoupled circuits from cells is best acceptable for a short time-scale when the cells are in their exponential phase of growth in nutrient rich medium. The long

term behavior of these synthetic circuits need to be studied and characterized as the applications that would rely on these circuits could span a longer period of time. This would require detailed analysis of how the cell behaves past the exponential phase and with increasing nutritional stress.

Thus far there have been limited studies on the long term behavior of synthetic networks and their stability under nutritional stress. It is a known fact that extra-chromosomal plasmids rely on the native cellular replication machinery which necessarily argues against the decoupling of synthetic and endogenous gene circuits. In the process of depending on the cell for its energetic and other requirements, synthetic gene circuits impose a metabolic burden on their cellular chassis. In order to better understand how synthetic gene circuits would behave in long term under changing environments including, but not limited to nutrient limitation, the following questions need to be answered

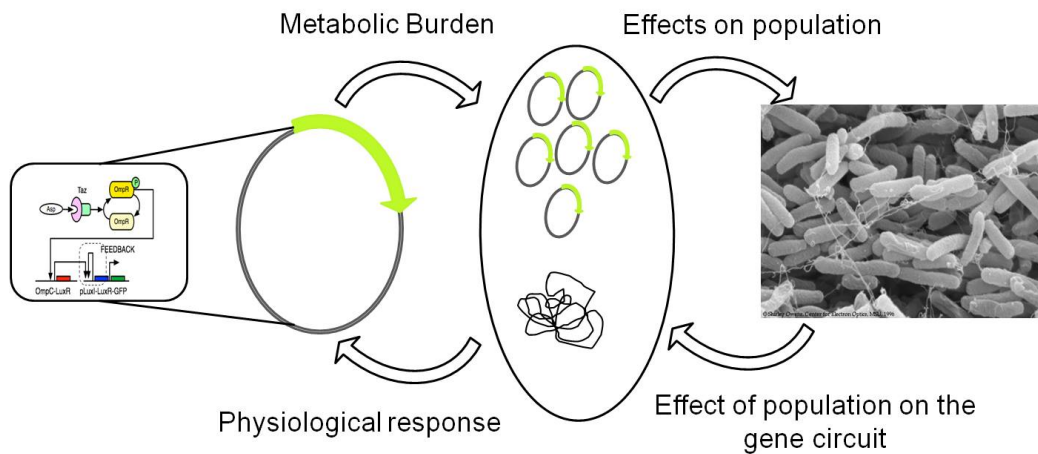


Figure 1.6. Behaviour of synthetic circuits in long-term experiments.

1. How does a gene circuit impose metabolic burden on the cell?
2. How does the cellular physiology change in response to the metabolic burden?
3. How do changes at the single cell level manifest at the population level?

4. How does the population dynamic modulate the apparent behavior of the gene circuit?

The central thesis of this project was to characterize how cells alter their physiology in response to increasing metabolic burden in long-term nutrient depleted culture conditions.

1.3 Physiological changes in a cell culture in response to metabolic burden

Microorganisms encounter stressful starvation-like conditions in their natural ecological niches which is unlike the resourceful growth they enjoy in laboratory cultures (44). A dynamic ecological equilibrium exists in nature where the microbes constantly evolve with time in order to survive an ever changing environmental landscape. Microbial adaptation to nutritional stress has been extensively addressed using *E. coli* as a model organism (44). An emerging conclusion from these studies is that starved cells undergo significant changes in physiology to help and metabolize alternate nutrients, which they otherwise would not use. This adaptive evolution is critical for cellular survival.

The canonical cell growth curve in Figure 1.7 distinguishes between four stages of cell growth namely- lag phase where the cells are adjusting to the environment, log phase where they grow exponentially using all the readily available nutrients, the stationary phase where the growth curve is equivalent to the death rate causing the curve to reach a stationary maximum value. At this stage the nutrients are scarce and soon after this stage the growth rate drops leading to the death phase.

In reality 99% percent of the cells die as they are rendered incapable of

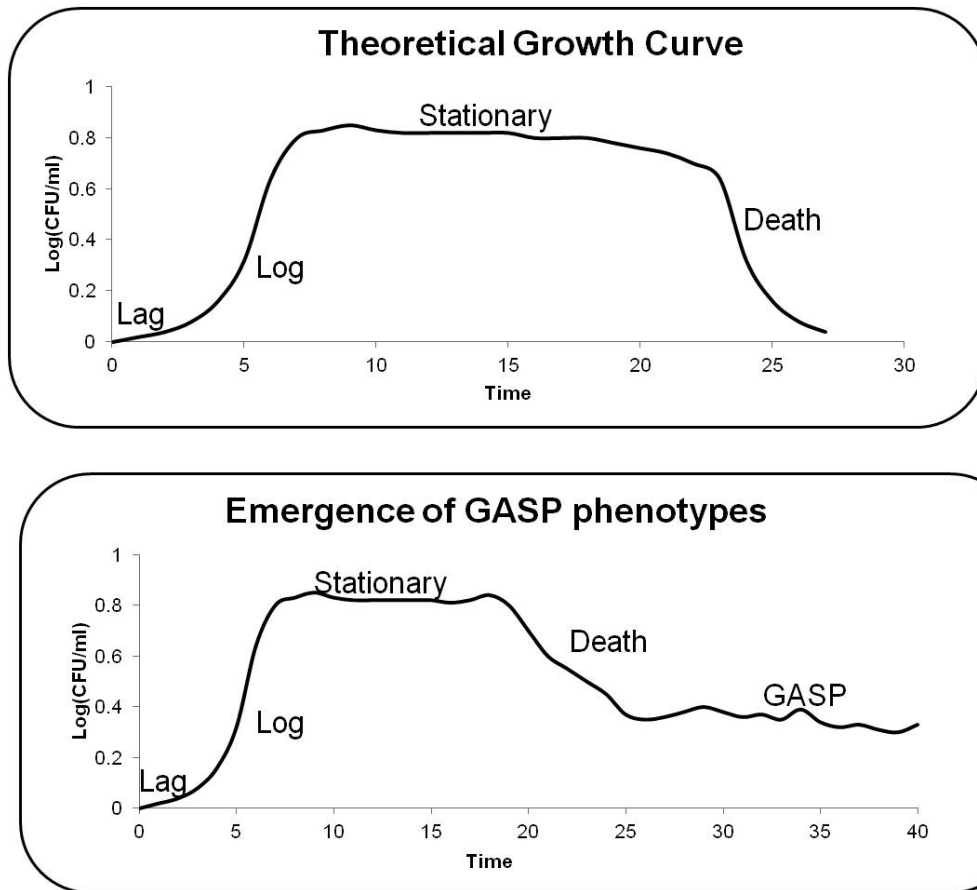


Figure 1.7. Growth curve graphs.
 Graphs showing the theoretical growth curve the emergence of GASP phenotypes after the death phase

carrying out repair and maintenance functions due to accumulation of oxidatively damaged proteins and nucleic acids (45). The remaining 1% of cells that manage to survive the death phase gain the ability to catabolize the remains of other cells to obtain amino acids from proteins, carbohydrates from the cell wall, lipids from cell membrane material and even information from DNA (46). This phase is called the *long term stationary phase*. The phenotype that emerges during this phase has a significant adaptive advantage and is called the Growth Advantage in Stationary Phase (GASP) phenotype (44; 47; 48; 49).

One of the hallmarks of the GASP phenotypes is ability of cells aged in long term batch cultures to outcompete cells from younger cultures (50). The cells

maintain the advantage even when subjected to repeated rounds of serial passage indicating that GASP phenotypes are heritable and are not just a temporary physiological adaptation (48). Four GASP mutations have been identified so far of which two loci have been well characterized (48; 49; 51; 52). The first mutation identified was in *rpoS*, which encodes the alternative sigma factor RpoS or σ^S . RpoS is a stationary phase-specific sigma factor responsible for global changes in gene expression at the onset of stationary phase mainly due to carbon starvation. RpoS regulates the physiological state of the cell by controlling the overall metabolism, pH, osmotic balance, temperature and oxidative stresses. (48; 49) The other mutation that has been studied has been mapped on the *lrp* which encodes the leucine- responsive protein (49; 51; 52). The activity of Lrp is controlled by the leucine levels within the cell. The Lrp regulon mainly includes genes responsible for amino acid metabolism and transport. Amino acid metabolism is regulated by Lrp regulin by increasing anabolism and decreasing catabolism (53; 54)

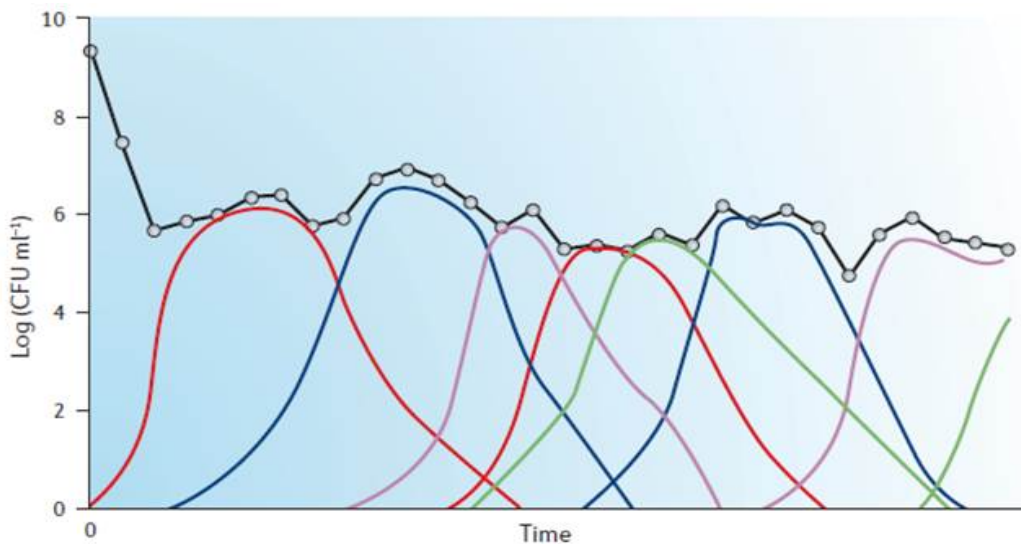


Figure 1.8. Dynamic emergence of GASP phenotypes (50).

The emergence of GASP phenotype is graphically depicted in Figure 1.6 that

quantifies cellular viability as log CFU/ml as a function of time. From the figure it can be seen that the net cellular viability remains constant through time. The emerging subpopulations represented by colored lines are the dynamically evolving GASP phenotypes which constantly displace the less fit siblings. The GASP phenotypes sweep through the population displacing remaining cells until it gets displaced by the next phenotype with increased fitness (47; 48; 55). There exists a genotypic homogeneity with functional diversity indicating the possible emergence of a dynamically evolving ecosystem (44).

Cells harboring synthetic gene networks on plasmids or as chromosomal integrants sustain significant metabolic burden. This in turn causes the host to rapidly uptake more nutrients than it would otherwise leading to quick exhaustion of available nutrients initiating the early onset of starvation like conditions. The lack of nutrients drive the cells to adapt to the nutrient-depleted environment by bringing about necessary physiological changes in order to thrive (56).

It has been observed and confirmed that adaptive phenotypes emerge as cells age (57; 58; 59; 60). These cells develop physiological changes that optimize cellular fitness empowering the cells to perform better even though growth rate is reduced owing to the increase in metabolic burden.

1.4 Specific aims of the project

In this research we investigate the potential use of cells exhibiting a GASP-like phenotype as a metabolically robust chassis for synthetic biology. GASP phenotypes are known to thrive under nutrient depleted condition unlike the naïve cells. Propagation and maintenance of the synthetic gene circuits adversely affect the cell's ability to grow and reproduce. GASP phenotypes being more resilient to harsher environments are more robust and could possibly

support synthetic gene networks over a longer time period. This fact makes GASP phenotypes ideal for applications where conditions cannot be controlled or monitored.

Specific aims of this project are described as follows

1. To reproduce the Growth Advantage in Stationary Phase (GASP) phenomenon - GASP phenotypes are more robust and contamination resistant. The aim to reproduce the GASP phenomenon is to test the consistency of its occurrence. This would be an indicator if these cells would be suitable as a chassis for synthetic biology. Recurrence of this phenomenon ensures reliable availability of these cells.
2. To analyze the metabolic burden imposed on cells due to the presence of plasmids- The presence of synthetic gene circuits imposes a metabolic burden. This aim would test the tolerance these cells would have to metabolic burden imposed on them.
3. To explore the effect of GASP on heterologous protein expression- This aimed at testing the ability of heterologous protein expression of the GASP phenotype as compared to the non-GASP phenotype.

The following chapters contain a detailed description of the experimental protocols followed and the results obtained.

Chapter 2

Materials and Methods

2.1 Growth conditions and media

All cultures experiments were performed in Luria-Bertani broth (LB) and M9 minimal media. The composition for LB media is listed below in Table 2.1. The ingredients were added to 1 l deionized water and autoclaved at 121°C and 15 psi. M9 minimal media was used in experiments to rule out any media dependency that the cells might have acquired. 5x M9 media solution was prepared as shown in Table2.2. The compounds were dissolved in 1 l water and autoclaved at 121 °C and 15 psi. 1x M9 media used in the experiments was made as mentioned in Table2.3. All the experiments were performed at 37°C unless otherwise mentioned. All antibiotics along with their concentrations used are listed in Table 2.4. All chemicals were purchased from Sigma-Aldrich (St. Louis, MO).

Table 2.1. Luria - Bertani broth

Ingredients	Quantity
Na ₂ HP0 ₄ .7H ₂ O	30 g
KH ₂ PO ₄	15 g
NaCl	2.5 g
NH ₄ Cl	5 g

Table 2.2. 5x M9 Minimal Media

Ingredients	Quantity
Na ₂ HP0 ₄ .7H ₂ O	30 g
KH ₂ P0 ₄	15 g
NaCl	2.5 g
NH ₄ Cl	5 g

Table 2.3. 1x M9 Minimal Media

Ingredients	Quantity
Sterile DI water	800 ml
M9 salts 5X stock solution	200 ml
Autoclaved 1M MgSO ₄	1 ml
Autoclaved 1M CaCl ₂	0.1 ml
Glucose	0.4%

Table 2.4. Antibiotics

Antibiotic	Concentration
Ampicillin	100 μg/l
Kanamycin	40 μg/l
Chloramphenicol	34 μg/l

2.2 Experimental methods and protocols

2.2.1 Absorbance and fluorescence assays

Growth curves were obtained by measuring the absorbance of the cells at OD₆₀₀ after sub-culturing an over-night at 1% dilution in fresh LB medium. Samples were transferred to a 96 well plate (Nalgene, Thermo-Scientific, NY) and the relative fluorescence (587/610 nm for mCherry and 515/528 nm for pVenus) and optical density at 600nm (OD₆₀₀) were measured using Tecan infinite M200 microplate reader. The fluorescence readings normalized as relative fluorescence units (RFU) with OD₆₀₀ absorbance to account for cell density. All experiments were performed in triplicates.

2.2.2 Fluorescence Activated Cell Sorting (FACS)

200 μ l cell sample from the 96 well plate was extracted and spun down at 15,000 rpm and re-suspended in 1 ml of 1x PBS with chloramphenicol and kept at 4°C until the samples were ready to be analyzed by Fluorescence Activated Cell Sorting (FACS). The MoFlo Sorter used for the experiment (Dako Cytomation, Ft. Collins, CO) is a multi-laser, high-speed sorter with multi-color analysis capability. The equipment was set to count 100,000 events. The lasers utilized on the equipment are green and yellow to excite the yellow fluorescent marker- pVenus and red fluorescent marker PmCherry respectively.

2.2.3 The *LacZ* competition experiment

The *LacZ* competition experiment served as the preliminary experiment to reproduce the GASP phenomenon. The cells used for this experiment were wildtype *E. coli* K12 MG1655 ($F^- \lambda^-$ ilvG- rfb-50 rph-1) cells. The basis for this experiment is that K12 cells could metabolize lactose due to the presence of an intact *lac* operon. Lac operon consists of three parts *lacZ*, *lacY* and *lacA* where *lacZ* encodes β -galactosidase. This enzyme degrades lactose into glucose and galactose which the cell can readily consume. In presence of 5-bromo-4-chloro-indolyl-galactopyranoside (X-gal) which is a lactose analog, β -galactosidase, enzyme product of the *lacZ* gene cleaves it to produce galactose and a dimerized indole ring that produces the characteristic blue color in colonies showing the presence of an intact *LacZ* gene.

The wild type strain with an intact *lac* operon was denoted as *LacZ+* . A *LacZ-* was constructed by P1 vir transduction of a kanamycin resistant gene cassette from BW2952 (F^- araD139 Δ (argF-lac) U169 rpsL150 deoC1 relA1 thiA ptsF25 flbB5301 rbsR malG:: λ placMu55 Φ (malG::*lacZ*)) to MG1655. The

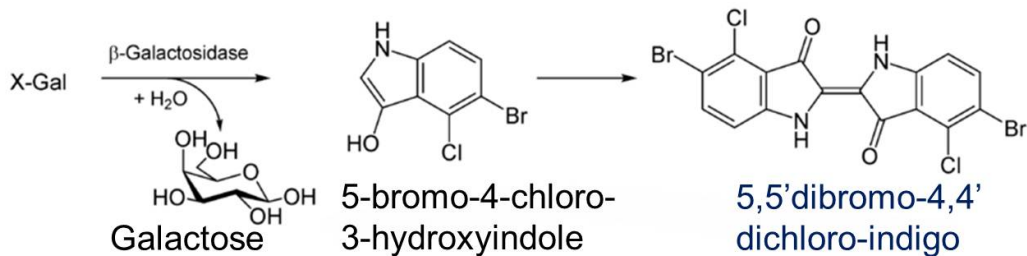


Figure 2.1. Action of β galactosidase. The enzyme cleaves Xgal into galactose and 5-bromo-4-chloro-3-hydroxyindole which immediately dimerizes to 5,5'-dibromo - 4,4' dichloro-indigo which gives blue color.

steps of lysate preparation and transduction are described below:

Lysate preparation and transduction

An overnight culture of the donor strain BW2952 possessing the kanamycin insert was made. The donor strain over night culture was diluted to a ratio of 1:50 into fresh LB medium with 5 mM $CaCl_2$ and 0.2% glucose. The subculture was grown for 1-2 hours until visible growth was observed. Few drops of the P1 phage lysate were added to the subculture and incubated for 3h until the cultures lysed. Chloroform was added to the lysate to kill the phage and thoroughly mixed. The cell debris was discarded by centrifugation and the lysate was stored at 4°C until further use. The recipient strain MG1655 was grown overnight in 4 ml LB. The overnight culture was centrifuged at 3000 rpm for 5m and resuspended in equal volume of fresh LB medium with 5 mM $CaCl_2$ and 100 mM $MgSO_4$. Two - three drops of donor P1 lysate prepared above were added and incubated at 37°C for 30-45 minutes. 200 μ l of 100 mM Na-citrate and 1 ml of LB medium was then added to the recipient strain and grown for 1.5-2 h. The cells were centrifuged at 3000 rpm for 5m and resuspended in 200 μ l fresh LB with 100 mM Na-citrate and spread on kanamycin selective plates and incubated overnight at 37°C. The *LacZ*- colonies obtained the following day were streaked

twice on plates containing kanamycin and sodium citrate to avoid phage contamination.

For selection purposes both these cell lines were transformed with pBR322 possessing both ampicillin and tetracycline resistance markers. *LacZ*⁺ and *LacZ*⁻ cells were aged by growing them for 40 hours in LB medium. OD₆₀₀ was measured every hour and aliquots were withdrawn every hour to make freezer stocks for further experiments.

Calibration of X-gal metabolism for *LacZ* experiment

The assay was developed to quantify the activity of the *LacZ* gene, which would serve as a proxy for the proportion of *LacZ*⁺ cells in a mixture of *LacZ*⁺ and *LacZ*⁻ cells. Traditionally X-gal the selection is used in solid cultures as a visual marker to aid selection of genetically engineered transformants. In order to use it in liquid cultures to identify the maximum activity of lac operon in presence of X-gal, following three quantities had to be determined-

1. The concentration of X-gal that could be used to differentiate between cells.
2. The time at which cells start metabolizing X-gal.
3. The wavelength where the dimerized indole ring would have maximum absorbance

Competition assay

Aged K12 cells were competed against younger cells to test which of the two would prevail. For this, freezer stock samples of *LacZ*⁺ and *LacZ*⁻ cells from hour 2 and hour 20 were selected.

Overnight cultures of *LacZ*⁺ and *LacZ*⁻ from hour 2 and hour 20 were grown in LB supplemented with ampicillin in 10 ml culture tubes. OD₆₀₀ of the overnight cultures were measured to ensure that it was similar and sub-cultured such that the OD for both the cells was approximately 0.02. The cells from *LacZ*⁺ hour 20 and *LacZ*⁻ hour 2 were mixed in a 1:1 ratio in two sets - one with 50% X-gal and other 0% X-gal. The experiment was also set with *LacZ*⁺ hour 2 and *LacZ*⁻ hour 20 as control. Point reads of OD were taken hourly after 6 hours of incubation. 10 μ l sample of cells was also plated on the agar plates containing ampicillin and X-gal every hour. These plates were incubated for 20 hours at 37°C.

2.2.4 Construction and aging of DH5 α cells for competition assay

The cells used in these set of experiments were *E. coli* DH5 α (F- endA1 glnV44 thi-1 recA1 relA1 gyrA96 deoR nupG Φ 80dlacZ Δ M15 Δ (lacZYA-argF) U169, hsdR17(*r*_K⁻ *m*_K⁺), λ -). For the ease of differentiating, cells were transformed with identical plasmids which differ only with respect to the fluorescent protein marker. The plasmids have a R6K origin, kanamycin resistance marker and mCherry and pVenus as the fluorescent reporter. These plasmids were kindly gifted by Prof. C.V Rao (ChBE, UIUC).

Overnight cultures of DH5 α cells was grown. 50 ml of LB media was inoculated in 1:100 dilution from the overnight culture and grown for 4h. They were spun down and washed with 10% glycerol three times. The DH5 α cells were then resuspended in 200 μ l 10% glycerol to make electrocompetent cells and stored at -80°C until further use.

Electrocompetent DH5 α were transformed with plasmids pVenus and

mCherry via electroporation to obtain the cell lines mC-DH5 α and pV-DH5 α . mC-DH5 α and pV-DH5 α cells were grown in 50 ml LB medium. Aliquots were withdrawn from these samples consecutively for the first three days to make freezer stocks. After the first three days aliquots were obtained every three days to make freezer stock samples. Along with making freezer stock, 10 ml of the sample was replaced by 10 ml of fresh LB media every three days to ensure the propagation of cells and to enrich any emergent GASP phenotypes. The samples were aged by growing for 15d.

2.2.5 Competition assay

Competition assay was conducted between samples from days 2, 12 and 15. Overnight cultures of mC-DH5 α and pV-DH5 α cell lines from days 2, 12, and 15 were started in LB under kanamycin selection. The OD₆₀₀ of the overnight cultures were measured and sub-cultured such that the OD for the cells was approximately 0.02. The competition assay was set up between aged pV-DH5 α cells and unaged mC-DH5 α cells and aged mC-DH5 α and unaged pV-DH5 α cells i.e. pV-DH5 α day2 with mC-DH5 α day 12 and mC-DH5 α day 15 and vice versa in 1:1 dilution. The whole experiment was set up on a 96 well plate with triplicates and conducted over 18h. The samples used for Fluorescence Activated Cell Sorter (FACS) were also set on the plate. Absorbance and fluorescence reading were taken by the spectrophotometer to monitor growth and fluorescence to monitor the expression of protein. The spectrophotometer was set at 37 °C with an orbital shaking set to 250rpm between reads. Hourly reads of absorbance and fluorescence were taken for 18h and samples for FACS were also withdrawn every three hours from the plate. These samples was spun down and resuspended in 1x PBS with cholramphenicol and stored at 4°C until ready to be analysed by flow cytometry. The genomic DNA from all the cells used for the competition

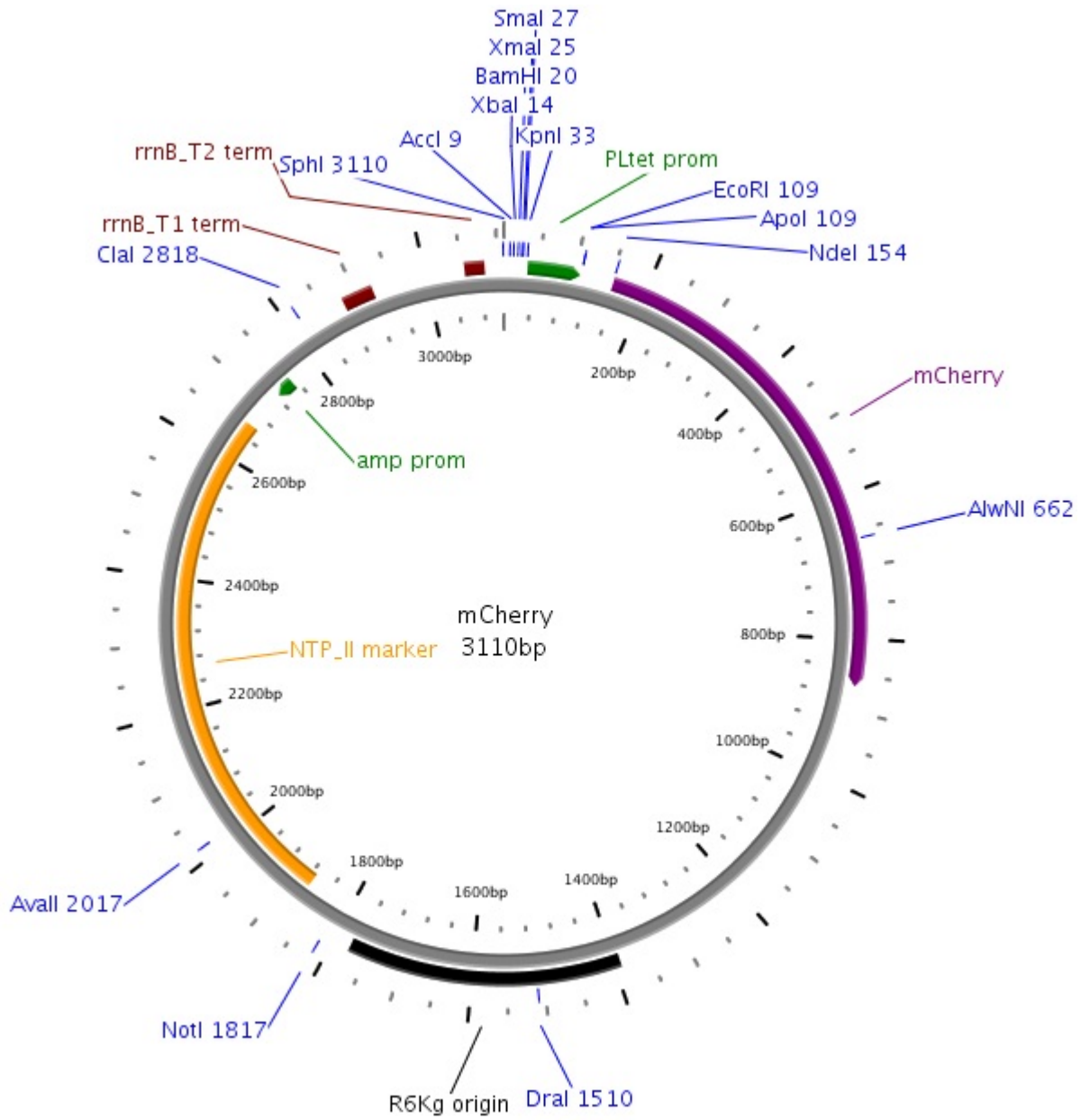


Figure 2.2. Plasmid map of mCherry.

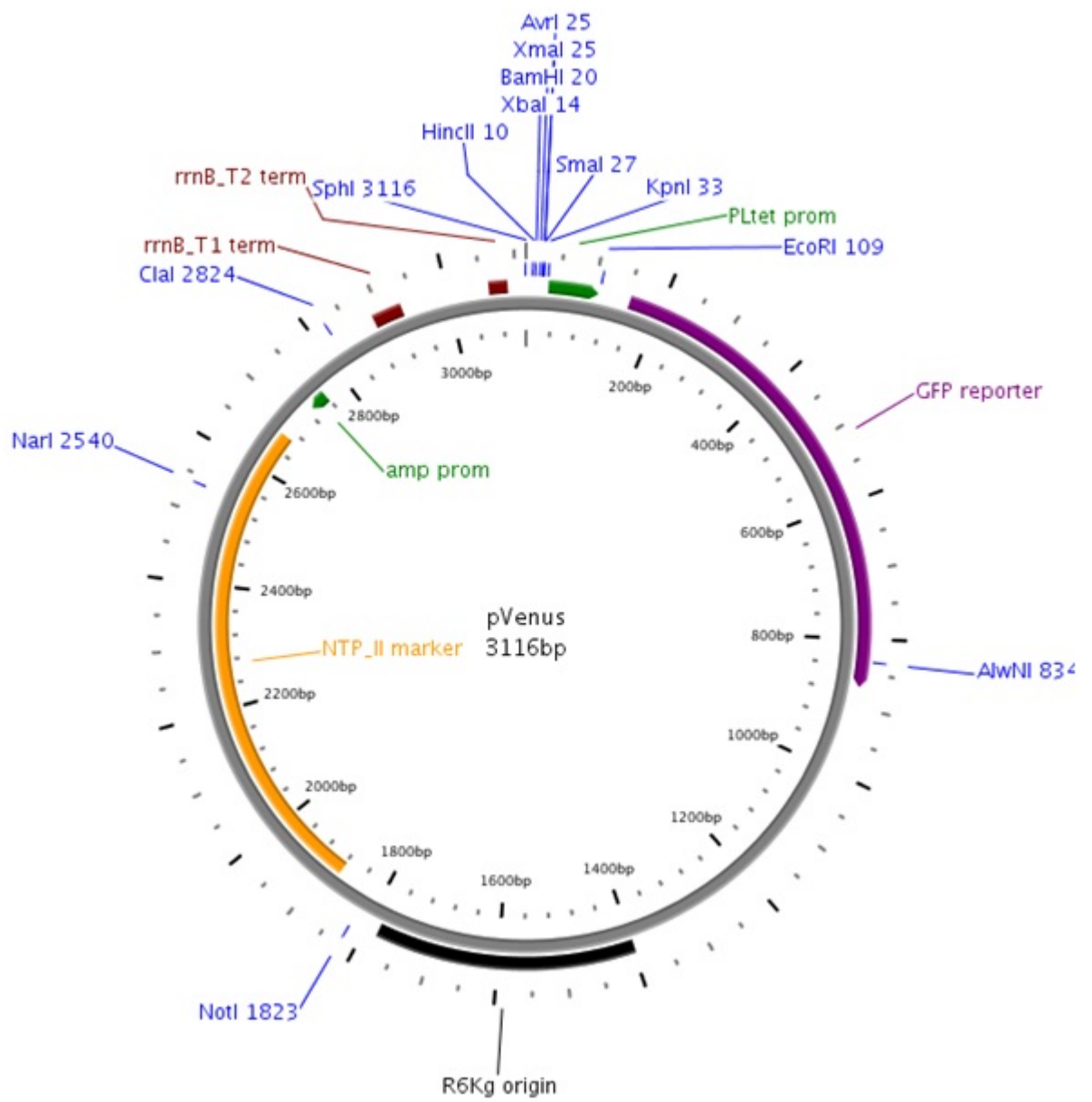


Figure 2.3. Plasmid map of pVenus.

assay was extracted and the *rpoS* was amplified using PCR and was sequenced.

2.2.6 Construction of cells with plasmids integrated in chromosome

Multiple copies of plasmids get reduced to a single copy when integrated in the chromosome. The method of integration used here is based on Conditional-Replication Integration and Modular (CRIM) system (61; 62). *E. coli* K12 MG1655 strains were used for this experiment.

E. coli K12 pir-pINT (J72008) cells were made electrocompetent (61). The electrocompetent K12 cells were transformed with mCherry fluorescent protein on a CRIM plasmid and pVenus fluorescent protein on CRIM plasmid via electroporation. These transformed cells were grown at 30°C on plate with kanamycin to select for cells with resistance. The pir-pINT helper plasmid has a temperature sensitive origin of replication due to which it is grown at 30 °C. During this incubation the CRIM plasmid replicates into multiple copies in presence of the pir protein. A single colony from the plate is picked and grown to saturation (OD₆₀₀ close to 1.6) in 5 ml LB medium with kanamycin at 37°C. The cells from the liquid culture were plated on agar plates with LB and kanamycin and incubated overnight at 43°C. This temperature cures the cell of the helper plasmid which has a temperature sensitive origin. From the plate at 43°C a single colony was picked and grown to saturation in 5 ml LB with kanamycin and plated on agar plates with LB and ampicillin to confirm the loss of helper plasmid since the helper plasmid has an ampicillin resistance marker. Cells were also plated on agar plates with LB and kanamycin for confirmation. Genomic DNA was isolated from the resulting colonies on the agar plate with kanamycin and analyzed to confirm integration of the CRIM plasmid. The ϕ 80 locus from

the chromosome was PCR amplified out to confirm the integration.

Assay for metabolic burden

The integrated cells, K12 with mCherry-RB01 and K12 with pVenus-RB02 were used to compare metabolic burden with mC-DH5 α and pV-DH5 α which were cells with plasmids. Overnight cultures of mC-DH5 α and pV-DH5 α and RB01 and RB02 were grown. These cells were sub-cultured in 1:100 dilutions. Absorbance at OD₆₀₀ was measured every 10 minutes for all the cell samples. The experiment was set up on a 96 well plate in triplicates. The data obtained for the growth curve was fit to the following logistic growth model for analysis.

$$y = \left(\frac{Asymptote}{1 + e^{\frac{X_{mid-input}}{scal}}} \right) \quad (2.1)$$

Where, *Asymptote* represents the maximum carrying capacity

Xmid represents represents the time taken to get to half of the asymptotic value

Scal is inversely proportional to the growth rate of the culture

The metabolic burden imposed on the cells by the plasmids was analysed by calculating the doubling time. Doubling time was compared with cells which had the construct integrated on chromosome.

2.2.7 Heterologous protein expression in GASP phenotype

The integrated cells, K12 with pmCherry -RB01 and K12 with pVenus -RB02 were aged in the same way as mC-DH5 α and pV-DH5 α and freezer stocks were made from them every three days. The naïve and day 15 cells of RB02 were transformed with PROTet 6xHN (Clontech, CA) plasmid with GFP (VP01) to observe expression. The naïve cells with this construct are referred to

as RB02G and the day 15 cells are referred to as RB02-15G The following steps were followed for the analysis.

Spectrophotometric analysis

The cells were grown overnight and diluted to 1:100 in fresh LB medium. The cells were then transferred to a 96 well plate in triplicates and grown at 37 °C in a spectrofluorometer for 18h. Through the period of 18h the growth curve and the fluorescence of the cells were monitored.

Western blot

The cells were grown overnight and diluted in 1:100 to in fresh LB medium and grown for 18 h. They were spun down and the lysates were analysed by western blot.

The reagents used for western blot were

- Transfer buffer (25 mM Tris base, 192 mM glycine)
- Tris buffer saline with Tween-20 or TBS-T (20 mM Tris pH 7.5, 0.8% w/v NaCl, 0.1% v/v Tween 20)
- Blocking buffer (TBS-T with 5% non fat dried milk)
- Primary antibody- anti GFP from goat aliquot stored in -20 °C, secondary antibody anti goat antibody from donkey stored at 4 °C, Electro Chemi Luminescence (ECL) Plus reagents stored at 4 °C (GE Healthcare, NJ)

The cells were subjected to Sodium Dodecyl Sulfate Polyacrylamide Gel Electrophoresis (SDS-PAGE) page at 250 V for 45m. PVDF transfer membranes and Whatman absorbent papers was cut to appropriate dimensions. The PVDF membrane was rinsed and soaked in 100% methanol, washed in DI water for 5m

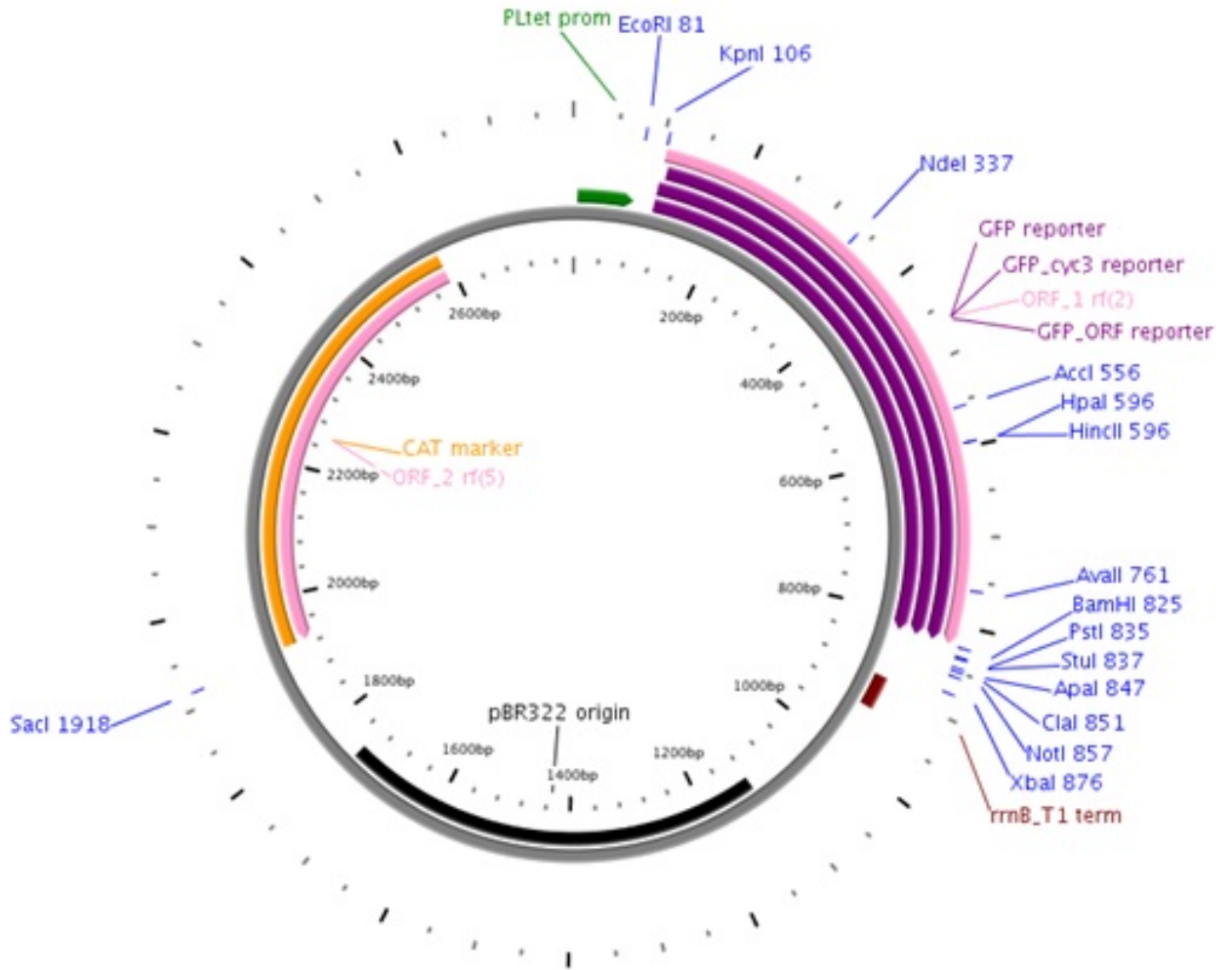


Figure 2.4. Plasmid map of PROTet 6x HNwith GFP. This plasmid construct was transformed into both RB02 naive and RB02 day 15 cells in order to study the heterologous protein expression.

and incubated in transfer buffer for 10m. The gel was incubated in transfer buffer for 10m. The absorbent papers and the fiber pads were also soaked in transfer buffer. The cassette was placed on a clean surface and the was arranged as in Figure 2.5.

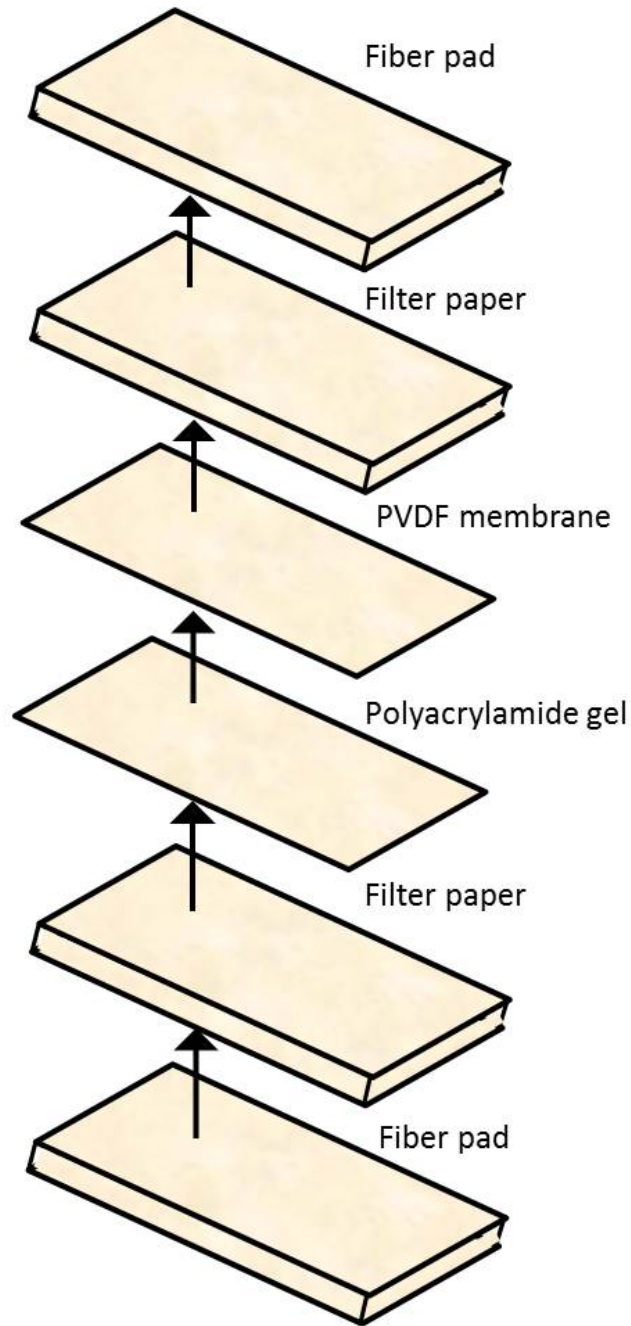


Figure 2.5. Assembly of the cassette for western blot.

The cassette was placed in the buffer tank and filled with chilled transfer buffer. This set-up was left over night at 4°C at 30 V with constant stirring. The membrane was retrieved from the cassette and incubated in 15 ml blocking buffer at room temperature with gentle shaking for 1h. The membrane was then rinsed with 20 ml TBS-T. The membrane was incubated in 20 ml TBS-T for 5 minutes with shaking. The buffer was discarded and the membrane was washed with TBS-T. 1:3000 dilution of anti GFP primary antibody was made in 30 ml of TBS-T and added to the membrane. The membrane was incubated with the antibody at room temperature for 1-2 h with gentle shaking. The membrane was rinsed with 20 ml TBS-T. The membrane was incubated with TBS-T for 5 minutes with gentle shaking and washed thoroughly. The membrane was washed 3 times every 5m with a change in buffer after every wash. The secondary antibody was diluted 1:5000 in 30 ml of TBS-T and incubated at room temperature with gentle shaking for 1 hour. The membrane was washed with 20 ml TBS-T and then incubated with 30 ml TBS-T and washed after 5m. The membrane was washed 3 times every 5m with a change in buffer after every wash to get rid of the excess antibody. ECL plus reagents were equilibrated to room temperature from 4°C. 4 ml of reagent A was mixed with 100 μ l of reagent B in a glass test tube wrapped in foil. The membrane was placed protein side up on a SaranTM wrap and the mixed ECL reagent was added to it. This was incubated at room temperature for 5m. After excess reagent was drained off a small amount of water was added to the scanning bed and the blot was placed protein side down for imaging.

Fluorescence Activated Cell Sorter (FACS)

The cells were grown overnight and diluted in 1:100 to in fresh LB medium and grown for 18 hours. The cells were washed in 1x PBS with ampicillin. These

cells were analysed on BD LSR II system (BD Biosciences) at an excitation
emmission of 490/525 nm.

Chapter 3

Results and Discussion

3.1 Reproducing the GASP phenomenon

3.1.1 *LacZ* competition experiment

The *LacZ* competition experiment served as a preliminary test to reproduce the GASP phenomenon. It was designed as a facile way to discriminate between GASP and non-GASP phenotypes by competing them for the same pool of resources. GASP and non-GASP phenotypes were discriminated on the basis of their ability to metabolize X-gal.

The calibration assay for identifying the maximum activity of *lac* operon in presence of X-gal showed that the cells did not show much difference between 30%, 40% and 50% Xgal. Figure 3.1 shows that the absorbance for the dimerized indole ring peaked between 640 nm and 650 nm so for all further experiments 645 nm was used as the wavelength and a concentration of 50% X-gal was used. The cells started consuming X-gal after the 5th hour when they were grown for 18h with 50% Xgal as shown in Figure 3.2.

Figure 3.3 shows the proportion of *LacZ*⁺ that could metabolize X-gal. The curves represent a mixture of *LacZ*⁺ and *LacZ*⁻ cells in varying proportions, starting with 0% *LacZ*⁺ to 100% *LacZ*⁺ cells. It can be seen that with the increase in proportion of *LacZ*⁺ cells the curve has a higher peak. Figure 3.3 was used as a calibration curve for the competition assay.

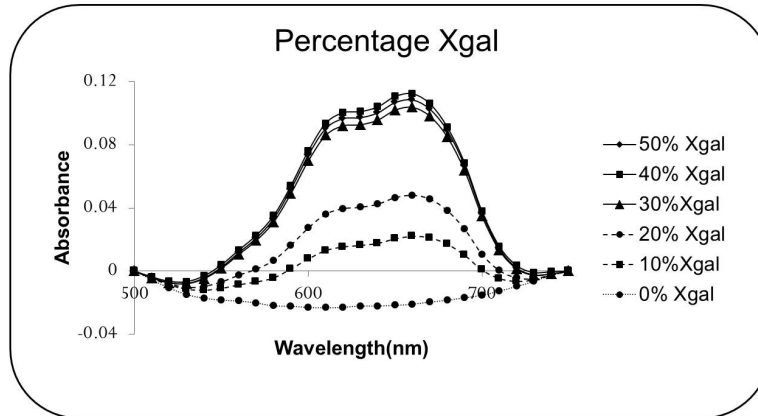


Figure 3.1. Colorimetric analysis of Xgal metabolism.

The *LacZ*⁺ cells were subjected to varying concentrations of Xgal. It can be observed that there is little difference between curves representing 30%, 40% and 50% Xgal.

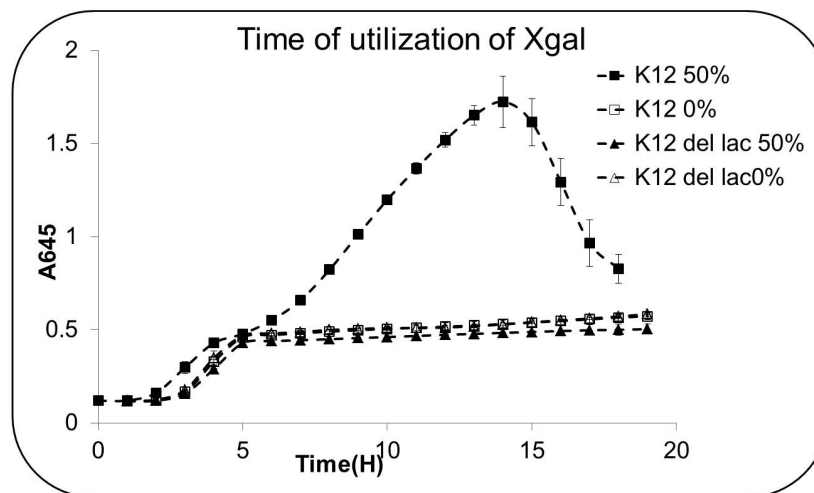


Figure 3.2. Calibration of Time.

Both *LacZ*⁺ and *LacZ*⁻ cells were grown in 0% and 50% Xgal. The *LacZ*⁺ cells in 50% Xgal show an increase in growth curve after the 5th hour.

Figure 3.4 shows results of competition assay between *LacZ*⁺ hour 20 and *LacZ*⁻ hour 2 and in 0% and 50% X-gal. It also shows the competition between *LacZ*⁺ hour 2 and *LacZ*⁻ hour 20 in 0% and 50% X-gal. When *LacZ*⁺20 and *LacZ*⁻2 cells were competed against each other in 1:1 ratio it was observed that *LacZ*⁺20 cells dominated. The calibration curves in Figure 3.3 was compared

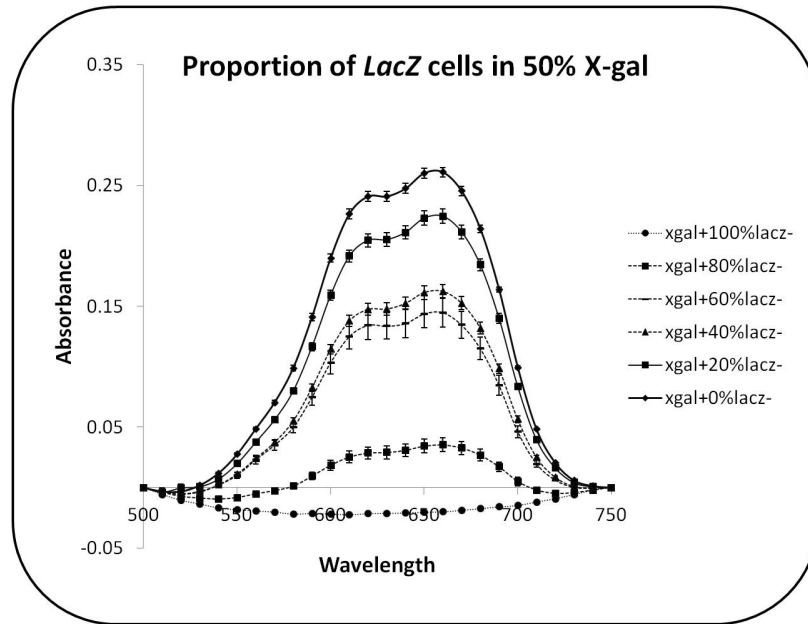


Figure 3.3. Proportion of *LacZ* cells in 50% X-gal. The graph represents the curves of mixed cultures of *LacZ* + and *LacZ* - cells in varying concentration. It can be seen that with the increasing concentration of *LacZ*+ the graph shows a higher curve.

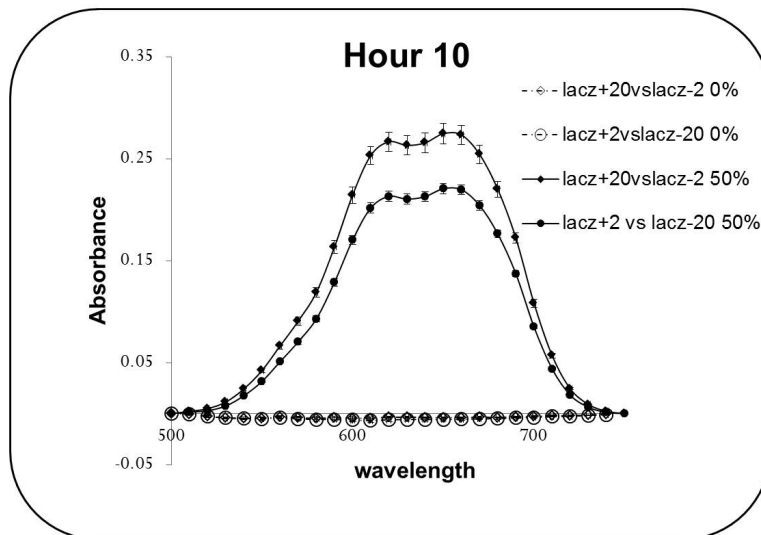
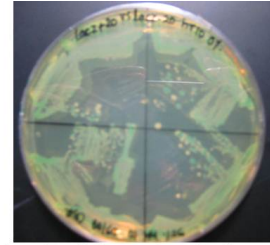
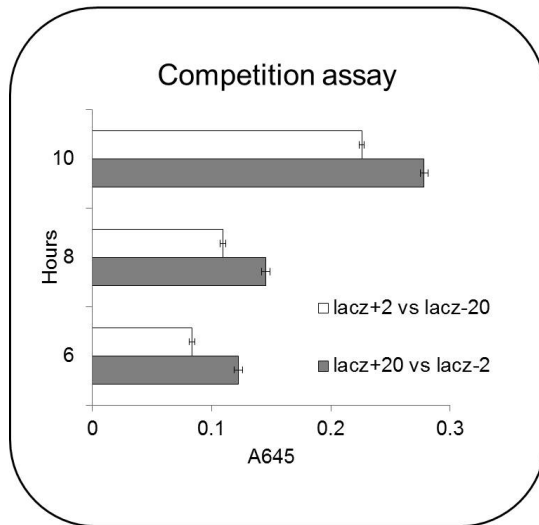
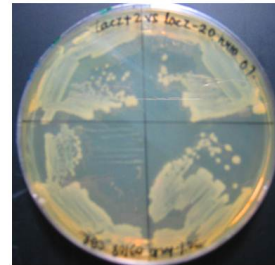


Figure 3.4. Competition assay results for *lacZ* cells. The results showed that the older cells prevail over the younger cells. The graph shows the result for boxing match between *LacZ*+ hour 20 and *LacZ*- hour 2 in 0% and 50% X-gal for hour 10.



LacZ+20 vs. LacZ-2 at hour 10



LacZ+2 vs. LacZ-20 at hour 10

Figure 3.5. Screening for GASP phenotype.

Image represents the colonies isolated from the assayed sample. The blue colonies in image of the plate *LacZ+20 vs. LacZ-2* at hour 10 dominate the plate. The white colonies observed in image of the plate *LacZ+2 vs. LacZ-20* at hour 10 indicate the domination of white colonies of the hour 20 *LacZ-* cells. Four colonies were plated on each plate for ruling out experimental errors.

with Figure 3.4 and it was observed that the curve representing *LacZ+20* and *LacZ-2* in 50% X-gal was in the same range as the 100% *LacZ+* cells. This showed that the *LacZ+20* cells dominated the population.

Absorbance in Figure 3.4 was normalized and the growth trend was subtracted from it so the exact ratio of cells that could metabolize X-gal could be identified. From the graph it can be inferred that the older cells *i.e* GASP phenotypes are able to metabolize X-gal faster.

The bar graph in Figure 3.5 shows that the aged cells dominated at all three time points (hour 6, 8 and 10) in 50% X-gal which seems to indicate that the GASP phenotypes that had emerged could metabolize X-gal faster and better than its younger counterparts. The 0% X-gal samples were used as a control for the competition assay. The control showed that in order to discriminate between

the *LacZ*+20 and *LacZ*-2 cells X-gal was necessary. The presence of X-gal introduced a media bias as only the *LacZ*+ cells could utilize it.

Single colonies that were isolated from these samples were plated on agar plates with LB containing ampicillin and X-gal. The image of the plate shows the older cells from hour 20 prevailing over the younger cells from hour 2. The plate with *LacZ*+20 and *LacZ*-2 showed larger proportion of blue colonies whereas the plate with *LacZ*+2 and *LacZ*-20 showed a larger proportion of white colonies further confirming that the aged cells dominate.

Conclusions of the *LacZ* experiment

GASP phenomenon was successfully reproduced. The GASP phenotypes tend to dominate in as few as 20 hours. The absence of *LacZ* renders the *LacZ*- cells unable to metabolize X-gal. This causes a media bias due to which aged *LacZ*- cells could not be accurately identified. Colony counting does not provide enough resolution to make conclusive inferences about the GASP phenotypes.

This preliminary experiment was improved upon by the Red-Green competition experiment. This experiment used cells with fluorescent protein markers, namely pmCherry and pVenus to distinguish between the GASP phenotype and non-GASP phenotype. FACS was used to analyse the samples which quantified the fluorescent cells accurately.

3.1.2 Quantification of competitive advantage of GASP phenotype

The cells constructed in section 2.2.4 were used for competition assay and the samples obtained from this experiment were analyzed using FACS which gave an accurate count of fluorescent cells of each type in a given sample. The

samples were simultaneously grown in LB and M9 media to ensure the phenomenon observed was not caused by media dependency.

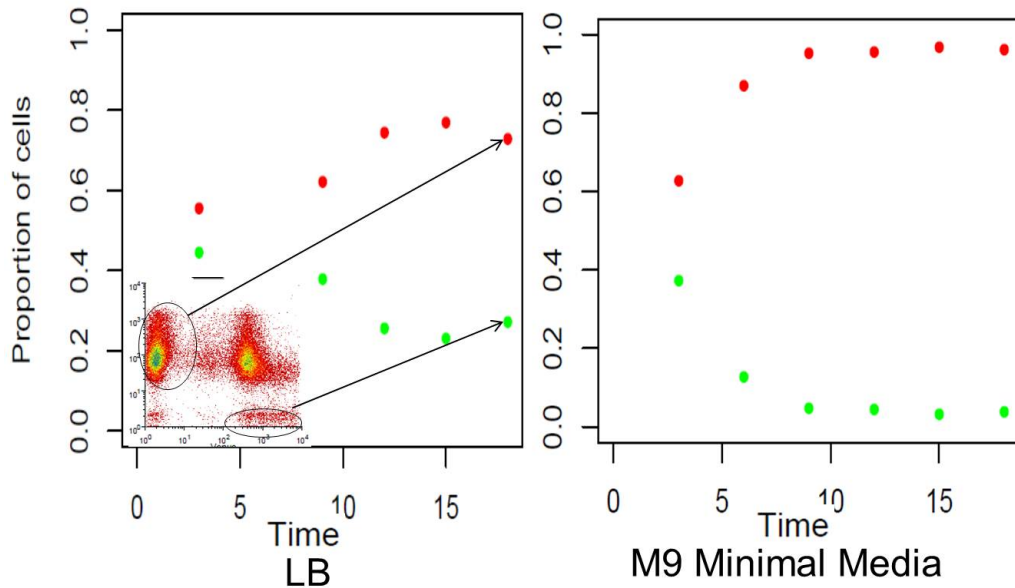


Figure 3.6. Competition assay results for DH5 α cells with fluorescent proteins. The day 15 PmCherry cells (solid red) out-competing the day 2 pVenus (solid green) in LB and same results are observed in M9 minimal media.

Figure 3.6 shows the results obtained from FACS analysis. The results showed that the aged cells out-competed the unaged cells.

Conclusions of the Red-Green fluorescence competition assay

The results from the Red-Green competition assay showed that the GASP phenotype dominated over the non-GASP phenotype. The DH5 α cells have *recA* deletion. The *recA* gene is responsible for triggering the SOS response in a cell which in turn triggers the activity of error prone nucleases thus enabling the cell to benefit from possible error prone mutations (63). Since DH5 α cells have *recA* deletion this should not occur. *rpoS* was sequenced from all the cells used for experiment- Day2, 12 and 15 of DH5 α -mCherry and DH5 α pVenus cells. This sequence showed no relevant mutation. Even though there is no *rpoS* mutation

GASP phenomenon is observed indicating that *rpoS* is not necessary for this phenomenon to occur.

GASP phenomenon successfully reproduced

GASP is a reproducible phenomenon and it is observed that GASP phenotype dominates over the non-GASP phenotype. This was confirmed by quantifying the competitive advantage that these cells had via FACS. GASP phenotypes could be exploited for synthetic biology as potential production platforms.

3.2 Analysis of metabolic burden

Doubling time is one of the indicators of how much metabolic burden is imposed on a cell. Higher metabolic burden increases the doubling time. Metabolic burden of the cells with plasmid were compared with that of the cells where the plasmids were integrated in the chromosome.

To quantify doubling time, growth curve data obtained was fit to the logistic growth model. Statistical programming language R was used to run this model.

$$y = \left(\frac{Asymptote}{1 + e^{\frac{Xmid - input}{scal}}} \right) \quad (3.1)$$

Where, *Asymptote* represents the maximum carrying capacity, *Xmid* represents represents the time taken to get to half of the asymptotic value, *Scal* is inversely proportional to the growth rate of the culture.

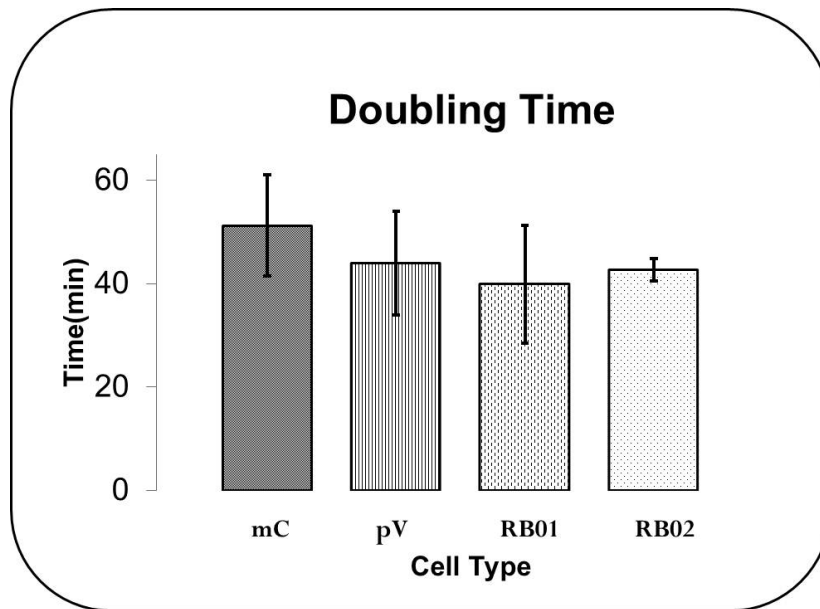


Figure 3.7. Doubling time calculated based on the Logistic growth model. The graph shows doubling time for DH5 α mCherry (mC), DH5 α pVenus (pV), K12mCherry (RB01) and K12pVenus (RB02). The plasmid based cells have a slightly doubling time indicating higher metabolic burden.

The values obtained from the model were used to plot Figure 3.7. Triplicate samples were fit to the model to yield the value plotted on the bar graph. It can be concluded from this experiment that cells with plasmids face higher metabolic burden as compared to cells where the plasmid has been integrated in the chromosome.

3.3 Heterologous protein expression in GASP phenotypes

This experiment was carried out to test the potential of GASP phenotypes as a production platform for commercially relevant proteins. For testing this GFP was used. There was approximately a two fold increase in the protein expression and these results were observed across two different transformations. The cells were tested in three ways - spectrophotometric analysis, western blotting, and FACS.

3.3.1 Spectrophotometric analysis

Growth curve of RB02 and RB02-15 were plotted along with normalized fluorescence. Figure 3.8 indicates that RB02-15 cells have a slower growth rate compared to RB02 cells. Figure 3.9 shows two fold increase in the expression of GFP.

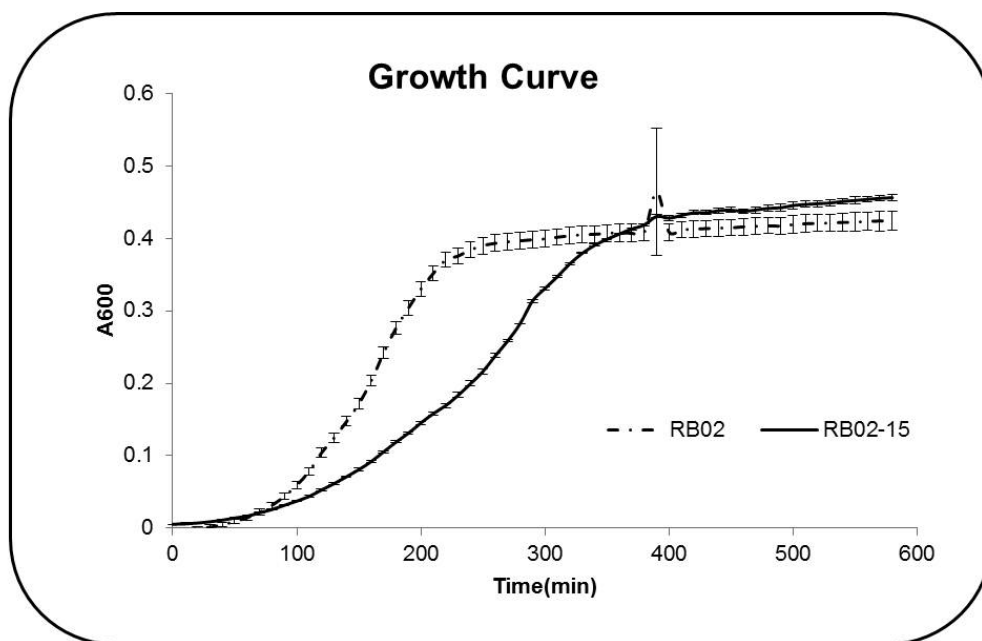


Figure 3.8. Growth curve of GASP phenotypes expressing GFP. The growth curve graph represents growth rate for RB02-G (dot and dash) and RB02-15 (solid line)

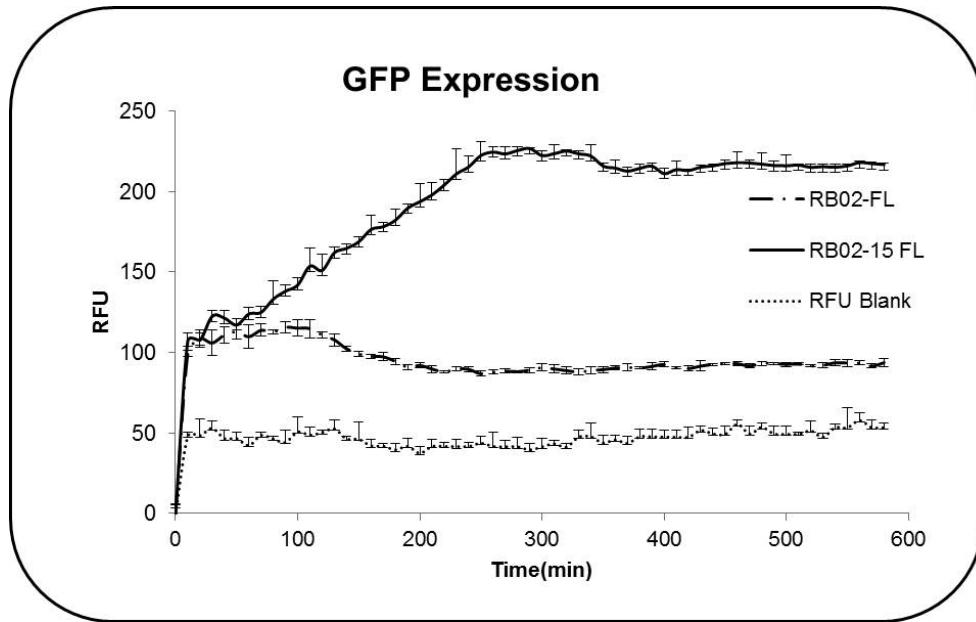


Figure 3.9. Spectrophotometric Analysis heterologous protein expression. The GFP expression graph represents R.F.U for RB02-G (dot and dash) and RB02-15G(solid line)

3.3.2 Western blot

Lysates from aged and naïve cells were blotted onto a polyvinylidene fluoride (PVDF) membrane and probed with anti-GFP antibodies. Band intensities were quantified to measure the relative amount of protein in each cell. Figure 3.10 indicates normalized band intensities. The RB02-15G shows 2 fold increase in the protein expression which is consistent with the spectrophotometric observations.

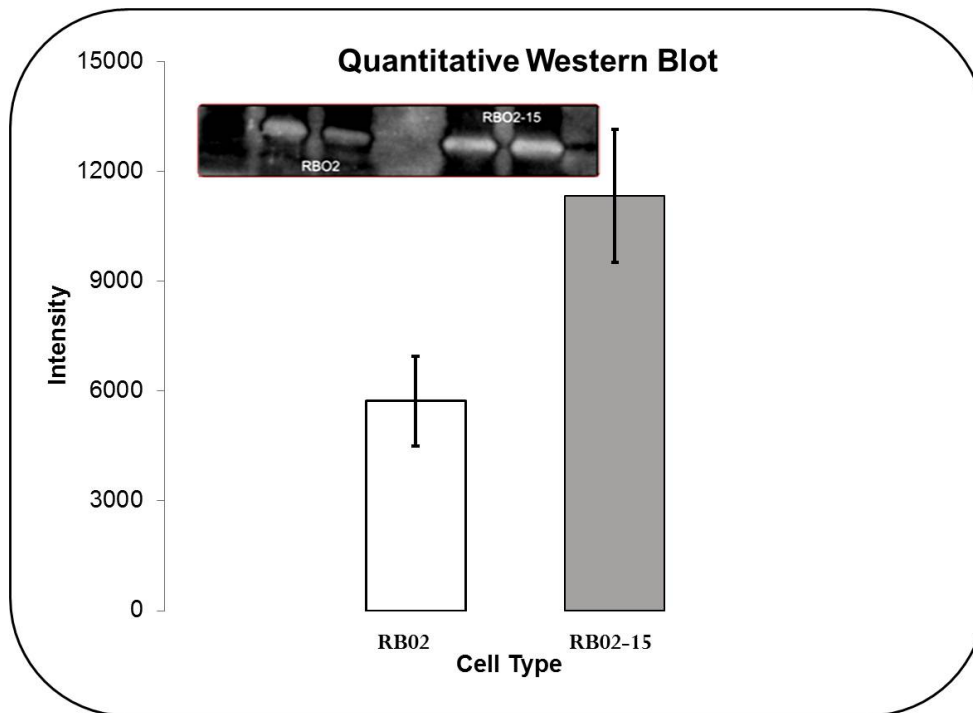


Figure 3.10. Quantitative western blot. The inset image for quantitative western shows the band from the PVDF membrane. The bar graph represents the intensities calculated from the membrane.

3.3.3 FACS analysis

FACS was done on the RB02 and RB02-15 cells to analyze the fluorescence per cell. The previous two methods quantified the total amount of protein which could be an average of fluorescing and non-fluorescing cells in the sample. This could be biased. FACS was used to rule out this ambiguity as it compared fluorescence per cell of the two cultures. The cells were subjected to FACS after 18h of growth. 100,000 events were counted on the FACS and the fluorescent events were counted and plotted. Figure 3.11 shows two fold increase in the expression of the protein.

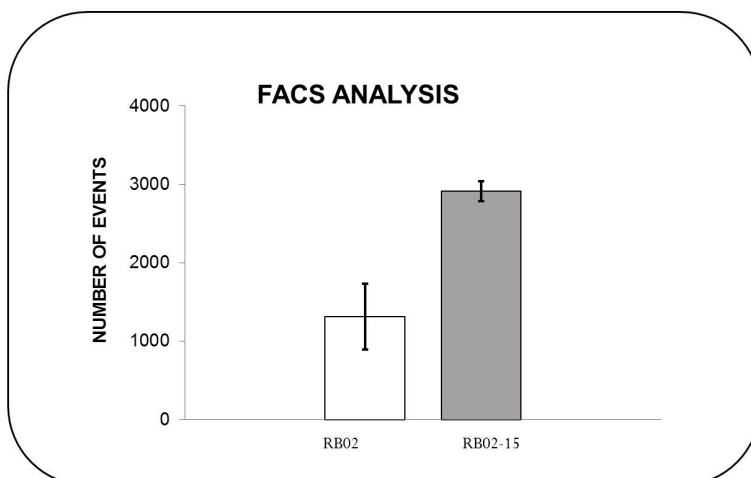


Figure 3.11. FACS analysis.

The graphs shows result for FACS where RB02-15G shows increase in expression.

Conclusion

The results observed for this experiment were really interesting, the aged cells showed higher expression as compared to naïve cells. Approximately two fold increase in expression of protein was observed in GASP phenotypes in comparison to non-GASP phenotypes. The fluorescence per cells was observed to increase as per the data from FACS and the growth rate. This increase in expression indicates the fact that the GASP phenotypes could be exploited as a chassis for production of proteins or other relevant compounds.

Table 3.1. Fold increase in expression

Method	Approximate Fold Increase
Kinetic on TECAN	2.3
Quantitative western blot	1.9
FACS	2.6

3.4 Conclusions

GASP phenotypes were observed in both experiments indicating that GASP phenomenon is reproducible through competitive assays. Competitive advantage of GASP phenotypes over naïve cells was quantified and the proportion of GASP cells were shown to increase with time indicating superior performance under nutrient deprived conditions. The robustness displayed by the GASP phenotype can most likely be attributed to the change in physiology of the cell. No mutations were observed in *rpoS* indicating that *rpoS* does not play an exclusive role in giving rise to GASP phenotypes. Cells with plasmids have a longer doubling time showing that cells with plasmids face higher metabolic burden. Furthermore, GASP phenotypes shows two fold increase in expression of heterologous protein. They have a slower growth rate, yet produce higher quantities of protein. Therefore, GASP phenotypes have a promising potential to serve as robust chassis for implementing synthetic biology circuits.

Chapter 4

Future Prospects

Since GASP phenotypes have shown to have a promising potential to serve as a robust chassis for synthetic biology circuits, it is essential that the physiology governing this phenomenon be examined in detail. The cause for increase in protein expression as a result of change in physiology needs to be investigated. The experiments in this project tested the expression of GFP, as a preliminary case. As the GASP phenotypes have a slower growth rate and an increased production of the protein it could significantly lower the production costs when scaled up. The expression of other commercially relevant proteins need to be tested in the GASP phenotypes to prove that these cells can indeed be used as a chassis for production of proteins, possibly at a commercial level.

References

- [1] Oltvai, Z. N. SYSTEMS BIOLOGY: Life's complexity pyramid. *Science* **298**, 763–764 (2002).
- [2] Csete, M. E. Reverse engineering of biological complexity. *Science* **295**, 1664–1669 (2002).
- [3] Goler, J. A., Bramlett, B. W. & Peccoud, J. Genetic design: rising above the sequence. *Trends in Biotechnology* **26**, 538–544 (2008).
- [4] Baker, D. *et al.* Engineering life: building a fab for biology. *Scientific American* **294**, 44–51 (2006).
- [5] Endy, D. Foundations for engineering biology. *Nature* **438**, 449–453 (2005).
- [6] Voigt, C. A. Genetic parts to program bacteria. *Current Opinion in Biotechnology* **17**, 548–557 (2006).
- [7] Canton, B., Labno, A. & Endy, D. Refinement and standardization of synthetic biological parts and devices. *Nature Biotechnology* **26**, 787–793 (2008).
- [8] Arkin, A. Setting the standard in synthetic biology. *Nature Biotechnology* **26**, 771–774 (2008).
- [9] Shetty, R. P., Endy, D. & Knight, T. F. Engineering BioBrick vectors from BioBrick parts. *Journal of Biological Engineering* **2**, 5 (2008).
- [10] Rosenfeld, N., Young, J. W., Alon, U., Swain, P. S. & Elowitz, M. B. Gene regulation at the single-cell level. *Science (New York, N.Y.)* **307**, 1962–1965 (2005).
- [11] Sleight, S. C., Bartley, B. A., Lieviant, J. A. & Sauro, H. M. In-Fusion BioBrick assembly and re-engineering. *Nucleic Acids Research* **38**, 2624–2636 (2010).
- [12] Weiss, R. & Thomas F. Knight, J. *DNA computing : 6th International Workshop on DNA-Based Computers, Leiden, the Netherlands, June 13-17, Pg1-8, 2000* (Springer, Berlin [u.a.], 2000).

- [13] Gardner, T. S., Cantor, C. R. & Collins, J. J. Construction of a genetic toggle switch in *Escherichia coli*. *Nature* **403**, 339–342 (2000).
- [14] Ptashne, M., Johnson, A. D. & Pabo, C. O. A genetic switch in a bacterial virus. *Scientific American* **247**, 128–130, 132, 134–140 (1982).
- [15] Elowitz, M. B. & Leibler, S. A synthetic oscillatory network of transcriptional regulators. *Nature* **403**, 335–338 (2000).
- [16] Nistala, G. J., Wu, K., Rao, C. V. & Bhalerao, K. D. A modular positive feedback-based gene amplifier. *Journal of Biological Engineering* **4**, 4 (2010).
- [17] Mitrophanov, A. Y. & Groisman, E. A. Positive feedback in cellular control systems. *BioEssays* **30**, 542–555 (2008).
- [18] Fuqua, C. & Greenberg, E. P. Signalling: Listening in on bacteria: acyl-homoserine lactone signalling. *Nature Reviews Molecular Cell Biology* **3**, 685–695 (2002).
- [19] Yao, G., Lee, T. J., Mori, S., Nevins, J. R. & You, L. A bistable *rb-e2f* switch underlies the restriction point. *Nature Cell Biology* **10**, 476–482 (2008).
- [20] Hasty, J., Dolnik, M., Rottschäfer, V. & Collins, J. Synthetic gene network for entraining and amplifying cellular oscillations. *Physical Review Letters* **88** (2002).
- [21] Stricker, J. *et al.* A fast, robust and tunable synthetic gene oscillator. *Nature* **456**, 516–519 (2008).
- [22] Lutz, H., R. & Bujard. Independent and tight regulation of transcriptional units in *Escherichia coli* via the LacR/O, the TetR/O and AraC/I1-I2 regulatory elements. *Nucleic Acids Research* **25**, 1203–1210 (1997).
- [23] Gibson, D. G. *et al.* Creation of a bacterial cell controlled by a chemically synthesized genome. *Science (New York, N.Y.)* **329**, 52–56 (2010).
- [24] Jones, D. T. & Woods, D. R. Acetone-butanol fermentation revisited. *Microbiological Reviews* **50**, 484–524 (1986).
- [25] Atsumi, S., Hanai, T. & Liao, J. C. Non-fermentative pathways for synthesis of branched-chain higher alcohols as biofuels. *Nature* **451**, 86–89 (2008).
- [26] Kirby, J. R. Synthetic biology: Designer bacteria degrades toxin. *Nature Chemical Biology* **6**, 398–399 (2010).

- [27] Haro, M. A. & de Lorenzo, V. Metabolic engineering of bacteria for environmental applications: construction of pseudomonas strains for biodegradation of 2-chlorotoluene. *Journal of Biotechnology* **85**, 103–113 (2001).
- [28] Skerker, J. M., Lucks, J. B. & Arkin, A. P. Evolution, ecology and the engineered organism: lessons for synthetic biology. *Genome Biology* **10**, 114 (2009).
- [29] Buffi, N. *et al.* Miniaturized bacterial biosensor system for arsenic detection holds great promise for making integrated measurement device. *Bioengineered Bugs* **2**, 296–298 (2011).
- [30] Martin, V. J. J., Pitera, D. J., Withers, S. T., Newman, J. D. & Keasling, J. D. Engineering a mevalonate pathway in escherichia coli for production of terpenoids. *Nature Biotechnology* **21**, 796–802 (2003).
- [31] Ro, D. *et al.* Production of the antimalarial drug precursor artemisinic acid in engineered yeast. *Nature* **440**, 940–943 (2006).
- [32] Dietrich, J. A. *et al.* A novel semi-biosynthetic route for artemisinin production using engineered substrate-promiscuous P450(BM3). *ACS Chemical Biology* **4**, 261–267 (2009).
- [33] Lu, T. K. & Collins, J. J. Engineered bacteriophage targeting gene networks as adjuvants for antibiotic therapy. *Proceedings of the National Academy of Sciences* **106**, 4629–4634 (2009).
- [34] Kohanski, M. A., Dwyer, D. J., Hayete, B., Lawrence, C. A. & Collins, J. J. A common mechanism of cellular death induced by bactericidal antibiotics. *Cell* **130**, 797–810 (2007).
- [35] Xiang, S., Fruehauf, J. & Li, C. J. Short hairpin RNA-expressing bacteria elicit RNA interference in mammals. *Nature Biotechnology* **24**, 697–702 (2006).
- [36] Wang, H. H. *et al.* Programming cells by multiplex genome engineering and accelerated evolution. *Nature* **460**, 894–898 (2009).
- [37] Bhalerao, K. Synthetic gene networks: the next wave in biotechnology? *Trends in Biotechnology* **27**, 368–374 (2009).
- [38] Lim, W. A. Designing customized cell signalling circuits. *Nature Reviews Molecular Cell Biology* **11**, 393–403 (2010).
- [39] Mukherji, S. & van Oudenaarden, A. Synthetic biology: understanding biological design from synthetic circuits. *Nature Reviews Genetics* (2009).

- [40] Sprinzak, D. & Elowitz, M. B. Reconstruction of genetic circuits. *Nature* **438**, 443–448 (2005).
- [41] Khalil, A. S. & Collins, J. J. Synthetic biology: applications come of age. *Nature Reviews Genetics* **11**, 367–379 (2010).
- [42] Lu, T. K., Khalil, A. S. & Collins, J. J. Next-generation synthetic gene networks. *Nature Biotechnology* **27**, 1139–1150 (2009).
- [43] Nandagopal, N. & Elowitz, M. B. Synthetic biology: Integrated gene circuits. *Science* **333**, 1244–1248 (2011).
- [44] Finkel, S. E. & Kolter, R. Evolution of microbial diversity during prolonged starvation. *Proceedings of the National Academy of Sciences of the United States of America* **96**, 4023–4027 (1999).
- [45] Nyström, T. Conditional senescence in bacteria: death of the immortals. *Molecular Microbiology* **48**, 17–23 (2003).
- [46] Finkel, S. E. & Kolter, R. Dna as a nutrient: novel role for bacterial competence gene homologs. *Journal of Bacteriology* **183**, 6288–6293 (2001).
- [47] Zambrano, M. GASPing for life in stationary phase. *Cell* **86**, 181–184 (1996).
- [48] Zambrano, M. M., Siegele, D. A., Almirón, M., Tormo, A. & Kolter, R. Microbial competition: Escherichia coli mutants that take over stationary phase cultures. *Science (New York, N.Y.)* **259**, 1757–1760 (1993).
- [49] Zinser, E. & Kolter, R. Escherichia coli evolution during stationary phase. *Research in Microbiology* **155**, 328–336 (2004).
- [50] Finkel, S. E. Long-term survival during stationary phase: evolution and the GASP phenotype. *Nature Reviews Microbiology* **4**, 113–120 (2006).
- [51] Zinser, E. R. & Kolter, R. Mutations enhancing amino acid catabolism confer a growth advantage in stationary phase. *Journal of Bacteriology* **181**, 5800–5807 (1999).
- [52] Zinser, E. R. & Kolter, R. Prolonged stationary-phase incubation selects for lrp mutations in escherichia coli k-12. *Journal of Bacteriology* **182**, 4361–4365 (2000).
- [53] Landgraf, J. R., Wu, J. & Calvo, J. M. Effects of nutrition and growth rate on lrp levels in escherichia coli. *Journal of Bacteriology* **178**, 6930–6936 (1996).

- [54] Calvo, J. M. & Matthews, R. G. The leucine-responsive regulatory protein, a global regulator of metabolism in *Escherichia coli*. *Microbiological Reviews* **58**, 466–490 (1994).
- [55] Finkel, S. E., Zinser, E. R., Gupta, R. & Kolter, R. Life and death in stationary phase. In *Molecular Microbiology*, vol. H 103, 3–16 (NATO-ASI Series, Series H: Cell Biology/Springer-Verlag., 1998).
- [56] Taymaz-Nikerel, H., van Gulik, W. M. & Heijnen, J. J. *Escherichia coli* responds with a rapid and large change in growth rate upon a shift from glucose-limited to glucose-excess conditions. *Metabolic Engineering* **13**, 307–318 (2011).
- [57] Elena, S. F. & Lenski, R. E. Microbial genetics: Evolution experiments with microorganisms: the dynamics and genetic bases of adaptation. *Nature Reviews Genetics* **4**, 457–469 (2003).
- [58] Lenski, R. E. Phenotypic and genomic evolution during a 20,000-Generation experiment with the bacterium *Escherichia coli*. In *Plant Breeding Reviews*, 225–265 (John Wiley & Sons, Inc., 2010).
- [59] Philippe, N., Crozat, E., Lenski, R. E. & Schneider, D. Evolution of global regulatory networks during a long-term experiment with *Escherichia coli*. *BioEssays* **29**, 846–860 (2007).
- [60] Shiloach, J., Reshamwala, S., Noronha, S. B. & Negrete, A. Analyzing metabolic variations in different bacterial strains, historical perspectives and current trends—example *E. coli*. *Current Opinion in Biotechnology* **21**, 21–26 (2010).
- [61] Anderson, J. C. *et al.* BglBricks: a flexible standard for biological part assembly. *Journal of Biological Engineering* **4**, 1 (2010).
- [62] Haldimann, A. & Wanner, B. L. Conditional-replication, integration, excision, and retrieval plasmid-host systems for gene Structure-Function studies of bacteria. *Journal of Bacteriology* **183**, 6384–6393 (2001).
- [63] Ennis, D. G., Fisher, B., Edmiston, S. & Mount, D. W. Dual role for *Escherichia coli* RecA protein in SOS mutagenesis. *Proceedings of the National Academy of Sciences of the United States of America* **82**, 3325–3329 (1985).